AD_____

Award Number: W81XWH-04-1-0189

TITLE: Role of Reactive Stroma in Prostate Cancer Progression

PRINCIPAL INVESTIGATOR: David R. Rowley, Ph.D.

CONTRACTING ORGANIZATION: Baylor College of Medicine
Houston TX 77030

REPORT DATE: February 2007

TYPE OF REPORT: Annual

PREPARED FOR: U.S. Army Medical Research and Materiel Command
Fort Detrick, Maryland 21702-5012

REPORT DOCUMENTATION PAGE

Form Approved
OMB No. 0704-0188

1. REPORT DATE *(DD-MM-YYYY)*	**2. REPORT TYPE**	**3. DATES COVERED** *(From - To)*
01-02-2007	Annual	12 Jan 04 – 11 Jan 07

4. TITLE AND SUBTITLE
Role of Reactive Stroma in Prostate Cancer Progression

5a. CONTRACT NUMBER

5b. GRANT NUMBER
W81XWH-04-1-0189

5c. PROGRAM ELEMENT NUMBER

6. AUTHOR(S)
David R. Rowley, Ph.D.

E-Mail: drowley@bcm.tmc.edu

5d. PROJECT NUMBER

5e. TASK NUMBER

5f. WORK UNIT NUMBER

7. PERFORMING ORGANIZATION NAME(S) AND ADDRESS(ES)

Baylor College of Medicine
Houston TX 77030

8. PERFORMING ORGANIZATION REPORT NUMBER

9. SPONSORING / MONITORING AGENCY NAME(S) AND ADDRESS(ES)
U.S. Army Medical Research and Materiel Command
Fort Detrick, Maryland 21702-5012

10. SPONSOR/MONITOR'S ACRONYM(S)

11. SPONSOR/MONITOR'S REPORT NUMBER(S)

12. DISTRIBUTION / AVAILABILITY STATEMENT
Approved for Public Release; Distribution Unlimited

13. SUPPLEMENTARY NOTES

14. ABSTRACT

The purpose of this project is to determine the role of FGF receptor 1 in reactive stroma during prostate tumorigenesis. We are using a novel approach to target transgene expression specifically to the reactive stroma of experimental prostate cancer. Using a modified approach, we are placing an inducible Cre recombinase behind the FAP gene promoter to target expression to reactive stroma. We will cross this mouse with Fgfr1flox mice (LoxP sites flanking FGF receptor 1 alleles). These mice will be crossed with TRAMP mice (prostate cancermodel). Induced expression of Cre at sites of reactive stroma generated in the cancer foci will function to excise the FGF receptor 1 alleles and create a conditional knockout mouse. Progression of tumorigenesis in this line of knockout mice will be compared to heterozygous and wild type controls. Progress has been made in each Task. We have completed all cloning steps and acquired all reagents. We have rederived the Fgfr1flox and have crossed it into the appropriate backgrounds. We have completed crossing the TRAMP mice with the Fgfr1flox mice. This study will pinpoint the role of FGF receptor 1 in reactive stroma promotion of prostate

15. SUBJECT TERMS
None provided

16. SECURITY CLASSIFICATION OF:			**17. LIMITATION OF ABSTRACT**	**18. NUMBER OF PAGES**	**19a. NAME OF RESPONSIBLE PERSON**
a. REPORT	**b. ABSTRACT**	**c. THIS PAGE**			USAMRMC
U	U	U	UU	46	**19b. TELEPHONE NUMBER** *(include area code)*

Table of Contents

W81XWH-04-1-0189 "Role of Reactive Stroma in Prostate Cancer Progression"

Introduction:

Considerable evidence now shows that a reactive stroma, similar to a wound repair stroma co-evolves with foci of prostate cancer. Our data indicates that stromal progenitor cells immediately adjacent to epithelial acini are activated to become the initial reactive stroma. This reactive stroma consists of activated fibroblasts and myofibroblasts. Our recent evidence supports the concept that overexpression of transforming growth factor beta one (TGF-β1) in carcinoma cells regulates the formation and biology of reactive stroma. Several growth factors in reactive stroma are TGF-β1 regulated. Our data shows that among these are connective tissue growth factor (CTGF) and fibroblast growth factor-2 (FGF-2) (1, 2). These studies have shown that attenuation of TGF-b signaling in carcinoma associated stroma resulted in decreased angiogenesis and rate of tumor growth. Of interest, TGF-b was shown to regulate message expression of both CTGF and FGF-2. Of particular interest, our most recent study has shown that TGF-b1 not only regulates protein expression but also stimulates release of the 18 kDa isoform of FGF-2 from prostate stromal cells (2). These studies have shown that xenograft tumors constructed with carcinoma cells and stromal cells with attenuated TGF-b signaling did not progress as rapidly as xenografts constructed with control stromal cells. Engineered expression of FGF-2 in the stromal cells with attenuated TGF-b signaling resulted in a recovery of rate of angiogenesis and xenograft growth rate. These studies show that FGF-2 is a key factor in mediating TGF-b mechanisms of action in prostate cancer associated reactive stroma. The focus of this application is to provide unique mouse models with which to probe mechanisms of FGF-2 action in the tumor microenvironment. Little is understood about signaling and the downstream mediators of FGF-2 action. Not only does FGF-2 regulate the tumor-associated stroma, but also there is emerging evidence that suggests that FGF-2 may mediate epithelial to mesenchymal transition of carcinoma cells during tumor progression to metastasis. Accordingly, completion of our proposed study will provide new models and new data on the specific responses and downstream pathways mediated by FGF-2 in tumor stroma.

Our project is based on the generation of a novel mouse model to knock out FGF-2 signaling in the reactive stromal compartment in order to address specific mechanisms and pinpoint those biologies specifically regulated by FGF-2 signaling. The expression of fibroblast activation protein (FAP) in the adult is restricted to reactive stromal cells (3, 4). We have proposed using the FAP gene to specifically target the expression of an inducible Cre recombinase to cancer associated reactive stroma. Three Specific Aims and Tasks were proposed that will generate a conditional knock out of the FGF receptor 1 gene (cognate receptor for FGF-2) in the reactive stroma tumor microenvironment of the TRAMP mouse model for prostate cancer. The use of the FAP-inducible Cre mouse will also benefit researchers studying other cancers, as FAP is generally expressed in reactive stroma of many different carcinomas.

Body:

Task 1 will knock-in DNA encoding the Mifepristone (RU 486) inducible Cre recombinase (CrePR1) into the fibroblast activation protein (FAP) locus.

This Aim is to generate a transgenic mouse that uses the FAP promoter to drive expression of an inducible Cre recombinase specifically to reactive stroma. It was our initial intent to use the FAP promoter and regulatory elements to target a Mifepristone-regulated Cre recombinase (CrePR1) expression specifically to reactive stroma. Recent studies have shown that the Mifepristone inducible system may be too leaky for our needs. Since FAP is expressed

Table of Contents

Figure 2: Alternative Approaches for Task 1

Task 1:

- Subcloning of 10 kb of FAP immediate upstream promoter from BAC clone containing the FAP gene.
- Acquisition of the tamoxifen inducible Cre recombinase.
- Gel purification of fragments.
- Ligation and cloning of construct.
- Verification of proper orientation and sequence fidelity.
- Provide verified construct to the GEM core.
- Characterization of founder mice and breeding to verify germ line transmission.
- Cross mice with ROSA reporter mice to verify induced expression in wound repair studies and leakiness in plus or minus tamoxifen conditions.
- Use mice for Task 2 and 3 experiments.

Task 2, is to cross these mice with a EF-1 / lox stop cassette / FGFR1 (dominant negative FGF receptor type I-myc tag) to create a FAP(CrePR1) / lox(stop) FGFR1 bigenic animal. **Modification approved in the previous Progress Report:** The *Fgfr1*^{flox} mouse will be used instead of the FGFR1 mouse for Task 2 in order to produce a conditional knockout.

The overall goal of Task 2 is to knockdown or knockout expression of FGF receptor I at sites of reactive stroma. As disclosed in the Previous Progress Report, we have recently generated an *Fgfr1*^{flox} mouse as part of this project. Instead of expressing the lox(stop) FGFR1 dominant negative to attenuate (knockdown) native gene expression, we decided to use a mouse that contains floxed alleles of the FGF receptor I (*Fgfr1*^{flox} mice) to fully knockout signaling. This is a much more straightforward approach to assure a conditional knockout of FGFR1 instead of expressing a competing dominant negative receptor. The *Fgfr1*^{flox} mice was provided to us by Juha Partanen (University of Helsinki, Finland) (5). As discussed in the previous Progress Report, we have spent the last 24 months rederiving this mouse (via embryo transfer) and crossing them from the ICR genetic background into the C57/BL/6 background. To date, we have made over 10+ generations of crosses and now have this mouse in the FVB and C57BL/6 background. Statistically, this has yielded *Fgfr1*^{flox} mice now in both the FVB and C57BL/6 background having less than 0.39% ICR background. This background is optimal for crossing with the FAP-Cre mice creating the bigenic FAP(Cre) / *Fgfr1*^{flox} (FVB) mouse line (heterozygous floxed FGFR1 allele). This step will complete Task 2. Figure 3 below shows the lines of mice and crosses to be made for each Task. In addition to the proposed experiments for Task 2, we have also generated a fibroblast cell line from the *Fgfr1*^{flox} mouse line peritoneum. Use of this cell line will aid us in extended studies to address specific signaling mechanisms.

Task 3, is to cross this bigenic animal with TRAMP mice. The TRAMP / FAP(CrePR1) / lox(stop) FGFR1 bigenic cross should exhibit RU 486 regulated expression of the dominant negative FGF receptor I transgene in TRAMP reactive stroma. **Modification approved in the previous Progress Report:** The resulting cross will produce the FAP(CrePR1) / *Fgfr1*^{flox} / TRAMP mouse that will result in RU 468 regulated FGF receptor I knockout in cancer associated reactive stroma (see Figure 3).

This Task will use the TRAMP (transgenic mouse prostate cancer). The TRAMP mouse uses the probasin minimal promoter to drive expression of SV40 large T antigen. Tumors occur when female TRAMP mice in the C57BL/6 background are crossed with male FVB breeders. The first step of Task 3 is to cross homozygous TRAMP mouse with the homozygous *Fgfr1*^{flox} (C57BL/6 background) mouse (generated in Task 2). This step has been completed. We have produced the TRAMP/ *Fgfr1*^{flox} line of mice in the C57BL/6 background and heterozygous for

floxed FGFR1 alleles and homozygous for TRAMP (first step in Task 3, see Figure 3 below). The next step in Task 3 will cross TRAMP/ *Fgfr1*^{flox} (C57BL/6) mice with the FAP(Cre)/ *Fgfr1*^{flox} (FVB) mouse generated in Task 2. This will yield [TRAMP/ *Fgfr1*^{flox} (C57BL/6)]/[FAP(Cre)/ *Fgfr1*^{flox} (FVB)] mice (Figure 3). Administration of tamoxifen to mice will induce the conditional knock out of FGFR1 alleles at sites of reactive stroma via tamoxifen-induction of Cre recombinase activity and removal of floxed alleles in FAP positive carcinoma associated stromal cells. Control tumors will be from TRAMP mice having heterozygous or wild type FGFR1 alleles and hence, functioning FGFR1. When exposed to Cre, a single allele knockout in heterozygous mice for floxed FGFR1 alleles showed a wild type phenotype in the previous studies of Partanen, which focused on developing mid- and hindbrain (5). Completion of Task 3 will produce data that will directly address the central hypothesis. Once our tamoxifen inducible Cre mouse is created, we will be able to rapidly proceed to Task 3. We anticipate completing this Task within the year of the no-cost extension.

Figure 3: Mouse lines generated in each Task

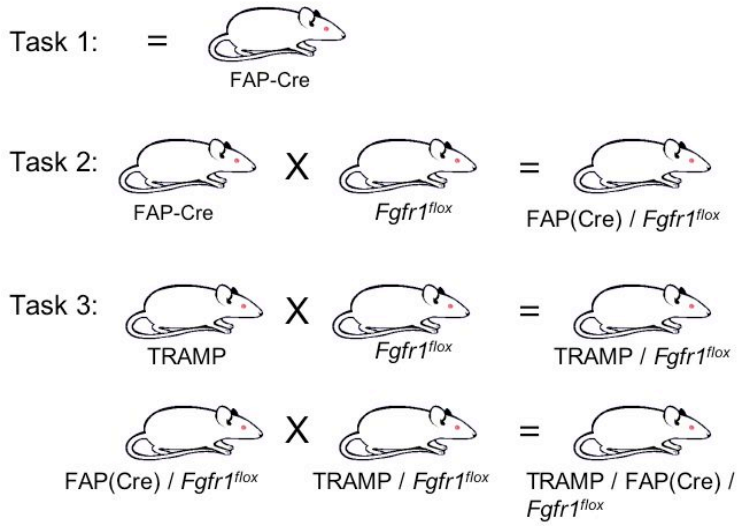

Key Research Accomplishments:

- Acquisition of BAC (clone RP23-161B24) containing the mouse FAP gene. Verification.
- Acquisition and subcloning of Mifepristone inducible Cre recombinase (CrePR1). Verification of sequence.
- Acquisition and subcloning of an SV40 Neo selection cassette flanked with Flp recombinase sites. Sequence verification.
- Construction and subcloning of a downstream IRES element. Sequence verification.
- Construction and subcloning of a downstream CrePR1. Sequence verification.
- Addition of a poly A tail downstream of CrePR1. Sequence verification.
- Step-wise construction and subcloning of flanking upstream and downstream 55 bp FAP gene sequence in reverse orientation (homologous to Exon 2 region of FAP gene). Sequence verification at each step for proper reverse orientation.
- Acquisition of EL250 cells containing an arabinose inducible *flpe* gene and all recombineering reagents.
- Acquisition of the *Fgfr1*^{flox} mice (ICR background) and confirmation of floxed alleles.
- Rederivation of the *Fgfr1*^{flox} mice by embryo transfer and initiation of *Fgfr1*^{flox} mice (ICR background) in TMF pathogen free facility.
- Acquisition of homozygous TRAMP mice and initiation of colony in TMF facility. Ready for crossing in Task 3.
- >8 generations of crossing *Fgfr1*^{flox} mice into FVB background. Now 0.39% ICR background. Ready for crossing Task 2 and 3.

- >8 generations of crossing *Fgfr1*^{flox} mice into C57BL/6 background. Now 0.39% ICR background. Ready for crossing in Task 2 and 3.
- 6 generations of crossing *Fgfr1*^{flox} mice with C57BL/6 (4 generations) and then crossing with TRAMP (2 generations). Now at less that 2% ICR background.
- Multiple experiments and conditions tested to recombine FAPupstream-IRES-CrePR1-FAPdownstream construct into BAC clones via homologous recombination.
- Acquisition and subcloning of tamoxifen inducible Cre recombinase as an alternative approach.
- Cloning of the 10 kb immediate 5' upstream mouse FAP promoter sequence as an alternative approach.

Reportable Outcomes:

During the previous Progress Period I provided an invited Chapter entitled "Reactive Stroma and Evolution of Tumors: Integration of Transforming Growth Factor-β, Connective Tissue Growth Factor, and Fibroblast Growth Factor-2 Activities" that discusses the role of FGF-2 signaling in cancer associated reactive stroma. This chapter is now at the Publisher and being completed. It will be included in the Textbook entitled: "Transforming Growth Factor-beta in Cancer Therapy" edited by Sonia B. Jakowlew at the NIH. This is both relevant to and supported by this project as this chapter discusses use of the FAP gene for targeting and the targeting of the FGF-2 signaling axis as a putative therapeutic.

- This chapter is now at the publisher and anticipated to be in press within the next 6 months. A draft of the chapter was provided in the last Progress Report.
- We published a manuscript in the previous Progress Period that addresses the role of CTGF in prostate reactive stroma biology (1). Publication of this data is relevant to this project as we show that TGF-β stimulates expression of both FGF-2 and CTGF in reactive stroma. This paper represents the CTGF arm of this regulation and the present project represents the FGF-2 signaling arm. The reprint is attached. Title: "Stromal expression of connective tissue growth factor promotes angiogenesis and prostate cancer tumorigenesis". The reprint is attached.
- During the last progress period, we have completed and submitted a manuscript that is now in review at Cancer Research. This manuscript is entitled "Fibroblast growth factor-2 mediates transforming growth factor beta action in prostate cancer reactive stroma". This work is directly relevant to the study. In this manuscript we show that attenuation of TGF-b signaling via either a conditional knockout or through expression of a dominant negative Smad3, results in a decreased angiogenesis and tumor growth rate with experimental prostate cancer xenografts. Of interest, we showed that FGF-2 message was up regulated by TGF-β1 in prostate stromal cells. Significantly, we showed that FGF-2 protein expression was stimulated by TGF-β1 and, significantly, the release of the 18 kDa isoform of FGF-2 was stimulated by TGF-β1. Finally, we showed that engineered re-expression of FGF-2 in stromal cells that were null for TGF-β receptor resulted in a restored angiogenesis and tumor growth. These data fully support the present project since it was our original hypothesis that FGF-2 signaling in cancer associated stroma promotes tumor growth. Generation of the engineered mouse lines from this study will allow us to probe specific mechanisms with novel models. The draft of the manuscript under review is attached.

Conclusions:

In this study we address the role of FGF receptor 1 signaling in carcinoma associated stroma by generating novel mouse models. A central goal here is the targeted gene expression specifically to sites of reactive stroma. The use of the FAP promoter is a novel concept and generation of the FAP(Cre) mouse will be a resource for all investigators who study reactive stroma tumor microenvironment, since FAP gene expression is observed in reactive stroma of all the major adenocarcinomas.

Although we have had major delays due to the inability to successfully recombine the engineered constructs into the BAC FAP locus, we have been able to focus the project using alternative approach techniques we believe will work much better. These approaches were disclosed as an alternative plan in the previous Progress Report. We are on track with these modifications and believe we can accomplish the study in the extended no cost period. We have acquired all the materials, clones and lines of cells and mice needed and have rederived them where necessary. We anticipate no further time delays in completing the study with the modified approach.

The proposed study will be the first time a transgene will be expressed specifically in the reactive stroma compartment of a tumor mouse model and represents the first time a gene will be conditionally knocked out in tumor associated stroma. This will make it possible, for the first time, to study the biology of engineered gene expression in the tumor microenvironment. These studies will permit the study of a microenvironment that was previously not possible. As an additional benefit, the FAP-Cre mouse will be valuable to other investigators using mouse models of cancer as the inducible Cre can be used to manipulate gene expression via either overexpression or attenuation of expression) gene expression. We are fully committed to completion of this project as we feel this will represent a major advancement.

References:

1. Yang, F., Tuxhorn, J. A., Ressler, S. J., McAlhany, S. J., Dang, T. D., and Rowley, D. R. Stromal expression of connective tissue growth factor promotes angiogenesis and prostate cancer tumorigenesis. Cancer Res, *65:* 8887-8895, 2005.
2. Yang, F., Strand, D., and Rowley, D.R. Fibroblast growth factor-2 mediates transforming growth factor-beta action in prostate cancer reactive stroma. Cancer Research, *(In Review)*, 2007.
3. Mathew, S., Scanlan, M. J., Mohan Raj, B. K., Murty, V. V., Garin-Chesa, P., Old, L. J., Rettig, W. J., and Chaganti, R. S. The gene for fibroblast activation protein alpha (FAP), a putative cell surface-bound serine protease expressed in cancer stroma and wound healing, maps to chromosome band 2q23. Genomics, *25:* 335-337., 1995.
4. Park, J. E., Lenter, M. C., Zimmermann, R. N., Garin-Chesa, P., Old, L. J., and Rettig, W. J. Fibroblast activation protein, a dual specificity serine protease expressed in reactive human tumor stromal fibroblasts. J Biol Chem, *274:* 36505-36512., 1999.
5. Trokovic, R., Trokovic, N., Hernesniemi, S., Pirvola, U., Vogt Weisenhorn, D. M., Rossant, J., McMahon, A. P., Wurst, W., and Partanen, J. FGFR1 is independently required in both developing mid- and hindbrain for sustained response to isthmic signals. Embo J, *22:* 1811-1823, 2003.

Stromal Expression of Connective Tissue Growth Factor Promotes Angiogenesis and Prostate Cancer Tumorigenesis

Feng Yang, Jennifer A. Tuxhorn, Steven J. Ressler, Stephanie J. McAlhany, Truong D. Dang, and David R. Rowley

Department of Molecular and Cellular Biology, Baylor College of Medicine, Houston, Texas

Abstract

Our previous studies have defined reactive stroma in human prostate cancer and have developed the differential reactive stroma (DRS) xenograft model to evaluate mechanisms of how reactive stroma promotes carcinoma tumorigenesis. Analysis of several normal human prostate stromal cell lines in the DRS model showed that some rapidly promoted LNCaP prostate carcinoma cell tumorigenesis and others had no effect. These differential effects were due, in part, to elevated angiogenesis and were transforming growth factor (TGF)-β1 mediated. The present study was conducted to identify and evaluate candidate genes expressed in prostate stromal cells responsible for this differential tumor-promoting activity. Differential cDNA microarray analyses showed that connective tissue growth factor (CTGF) was expressed at low levels in nontumor-promoting prostate stromal cells and was constitutively expressed in tumor-promoting prostate stromal cells. TGF-β1 stimulated CTGF message expression in nontumor-promoting prostate stromal cells. To evaluate the role of stromal-expressed CTGF in tumor progression, either engineered mouse prostate stromal fibroblasts expressing retroviral-introduced CTGF or 3T3 fibroblasts engineered with mifepristone-regulated CTGF were combined with LNCaP human prostate cancer cells in the DRS xenograft tumor model under different extracellular matrix conditions. Expression of CTGF in tumor-reactive stroma induced significant increases in microvessel density and xenograft tumor growth under several conditions tested. These data suggest that CTGF is a downstream mediator of TGF-β1 action in cancer-associated reactive stroma and is likely to be one of the key regulators of angiogenesis in the tumor-reactive stromal microenvironment. (Cancer Res 2005; 65(19): 8887-95)

Introduction

Our previous studies have characterized reactive stroma in human prostate cancer progression and have developed the differential reactive stroma (DRS) xenograft model to address the role of reactive stroma in experimental prostate tumorigenesis. These studies have shown that reactive stroma initiates during prostatic intraepithelial neoplasia, exhibits a myofibroblast wound repair stromal phenotype, is tumor promoting, and is mediated, in part, by transforming growth factor (TGF)-β1 action (1–3). Our studies have also shown that reactive stroma was essential for inducing early angiogenesis and acted to stimulate both the incidence and rate of LNCaP prostate cancer cell tumorigenesis in DRS model xenografts (2). These studies showed that differential LNCaP tumor progression is based on the type of stroma in the xenograft tumor and the stromal response to TGF-β1.

Connective tissue growth factor (CTGF) has emerged as a potent mediator of TGF-β1 action in wound repair stromal responses and in fibrosis disorders (4–6). CTGF is a member of the CCN gene family (for CTGF, Cyr61, and Nov; refs. 7–9). This family includes six structural and functional related proteins: CTGF (10, 11); cysteine-rich 61 (Cyr61; ref. 12); nephroblastoma overexpressed (NovH; ref. 13); and Wnt-1–induced signaling protein (WISP) 1, WISP2, and WISP3 (14). The CCN family members (excluding WISP2) share four conserved structural modules with sequence homologies similar to insulin-like growth factor–binding protein, von Willebrand factor, thrombospondin, and cysteine knot (8). CTGF message is potently stimulated by TGF-β1 (15–19) and likely mediates TGF-β1–induced collagen expression in wound repair fibroblasts (20). CTGF is expressed by several stromal cell types, including endothelial cells, fibroblasts, smooth muscle cells, and myofibroblasts, and some epithelial cell types in diverse tissues. Consistent with its role in connective tissue biology, CTGF enhances stromal extracellular matrix synthesis (16) and stimulates proliferation, cell adhesion, cell spreading, and chemotaxis of fibroblasts (10, 16, 21). CTGF was also shown to stimulate smooth muscle cell proliferation and migration (22). In addition, CTGF is a potent stimulator of endothelial cell adhesion, proliferation, migration, and angiogenesis *in vivo* (23–25). As might be predicted, CTGF is expressed in the reactive stromal compartment of several epithelial cancers, including mammary carcinoma, pancreatic cancers, and esophageal cancer (26–28). Expression of CTGF is also observed in several stromal cell disorders, including angiofibromas, infantile myofibromatosis, malignant hemangiopericytomas, fibrous histiocytomas, and chondrosarcomas (29, 30). Accordingly, CTGF is considered to be a profibrosis marker (31). Together, these findings suggest that CTGF is a key regulatory factor for stromal tissue biology in wound repair and cancer progression; however, this has not yet been tested *in vivo* using engineered stromal cells.

Expression of TGF-β1 is elevated in most epithelial carcinoma cells (32) and our previous studies have shown that TGF-β1 is a critical regulator of carcinoma-associated reactive stroma, angiogenesis, and reactive stroma promotion of tumor progression in LNCaP xenograft tumors (3). Because TGF-β1 stimulates CTGF expression in stromal cells (15), including human prostate stromal cells (19), CTGF has accordingly emerged as a candidate downstream effector of TGF-β1 action in reactive stroma.

The DRS model system was specifically developed to evaluate differential gene expression in the reactive stromal compartment

Note: J.A. Tuxhorn is currently in Life Sciences Systems and Services, Wyle Laboratories, Houston, TX 77058.

Requests for reprints: David R. Rowley, Department of Molecular and Cellular Biology, Baylor College of Medicine, One Baylor Plaza, Houston, TX 77030. Phone: 713-798-6220; Fax: 713-790-1275; E-mail: drowley@bcm.tmc.edu.

doi:10.1158/0008-5472.CAN-05-1702

in xenografts composed of tissue-specific cancer cells and coordinate stromal cells (2, 3). These studies showed that two different human prostate stromal cell lines, HTS-2T and HTS-40C, exhibited differential effects in reactive stroma-induced angiogenesis and tumorigenesis of LNCaP prostate cancer cells (2). The present study was conducted to assess candidate genes responsible for the differential functions. We report here that CTGF was differentially expressed in tumor-promoting prostate stromal cell lines and that CTGF expression is stimulated by TGF-β1 in prostate stromal cells. In addition, we show that overexpression of CTGF in engineered prostate stromal cells in the DRS LNCaP xenograft model resulted in significantly elevated angiogenesis and LNCaP tumorigenesis *in vivo*.

Materials and Methods

Cell lines. LNCaP human prostate carcinoma cells were purchased from American Type Culture Collection (ATCC, Manassas, VA) and maintained in RPMI 1640 (Invitrogen, Carlsbad, CA) supplemented with 10% fetal bovine serum (FBS, Hyclone, Logan, UT), 100 units/mL penicillin, and 100 μg/mL streptomycin (Sigma, St. Louis, MO). The HTS-2T and HTS-40C normal human prostate stromal cell lines were established in our laboratory (2) and cultured in Bfs medium: DMEM (Invitrogen) supplemented with 5% FBS (Hyclone), 5% Nu serum (BD Biosciences, Bedford, MA), 0.5 μg/mL testosterone, 5 μg/mL insulin, 100 units/mL penicillin, and 100 μg/mL streptomycin (Sigma). The Phoenix E packaging cell line was received from ATCC (by permission from Dr. Gary Nolan, Stanford University, Stanford, CA) and maintained in DMEM with high glucose (Invitrogen) supplemented with 10% heat inactivated FBS (Hyclone), 2 mmol/L glutamine (Invitrogen), and antibiotics as described above.

The mouse prostate stromal cell line, C57B, was derived from an 8-week C57BL/6 male mouse. The ventral prostate was removed, cut into 1 mm^3 cubes, and placed in wells of a six-well culture plate in Bfs medium and cultured at 37°C with 5% CO_2. Monolayers of stromal cells extended from the explants and, at confluence, the explants were removed and stromal cells were continued in culture by routine serial passage. C57B cells were positive for androgen receptor, vimentin, and smooth muscle α-actin with low expression of calponin (data not shown), similar to human prostate stromal cell lines we have reported previously (2). C57B cells were used at passages 15 to 25 for all experiments.

The GeneSwitch-3T3 cell line expressing the GeneSwitch regulatory protein from the pSwitch vector was purchased from Invitrogen. GeneSwitch-3T3 cells and derivative engineered cell lines were maintained in DMEM (Invitrogen) supplemented with 10% FBS (Hyclone), 100 units/mL penicillin, 100 μg/mL streptomycin (Sigma), and Hygromycin B and/or Zeocin (Invitrogen) as described below.

cDNA microarray analysis. HTS-2T and HTS-40C cells were cultured in Bfs medium to 80% confluence. Total RNA was extracted from each cell line with RNA STAT-60 total RNA/mRNA isolation reagent (Tel-test, Inc., Friendswood, TX) following the instructions of the manufacturer. Microarray analysis was done using 30 μg of total RNA. The cDNA reverse transcription and fluorescent labeling reactions were carried out using Cy3-labeled nucleotides for control (HTS-2T) and Cy5-labeled nucleotides for experimental (HTS-40C) samples as described previously (33). A microarray chip carrying 6,000 human cDNAs obtained from Baylor Microarray Core Facility was used. The hybridized slide was scanned with an Axon 4000A dual-channel scanner (Axon Instruments, Foster City, CA) and the data was analyzed using Gene Pix v. 3.0 software package (Axon). Genes were considered up-regulated if the expression was changed at least 3-fold from the control. Data with low signal intensity, high background, and high variability were eliminated.

Reverse transcription-PCR. Differential expression of CTGF in HTS-2T and HTS-40C cells was assessed by reverse transcription -PCR (RT-PCR) analysis. HTS-2T and HTS-40C cells were cultured in Bfs medium to 80% confluence and total RNA was extracted with the RNeasy Miniprep kit (Qiagen, Inc., Valencia, CA). CTGF amplification with primer 5′-GGTTACCAATGACAACGCCT-3′ and primer 5′-TGCTCCTAAAGCCACACCTT-3′ were used to monitor CTGF expression, by using the TaqMan one-step RT-PCR kit (Applied Biosystems, Foster City, CA).

To determine the effects of TGF-β1 on CTGF expression, HTS-2T cells were cultured to 80% confluence, exposed to M_0 serum-free media (MCDB 110 supplemented with insulin, transferrin, and sodium selenite; Sigma Diagnostics) for 24 hours, followed by 100 pmol/L (2.5 ng/mL) porcine TGF-β1 (R&D Systems, Minneapolis, MN) or vehicle control in M_0 media treatment for an additional 24 hours before total RNA extraction as described above. 18S rRNA amplifications with 18S rRNA primers (provided in the TaqMan one-step RT-PCR kit) were used for total RNA loading control. RT-PCR reactions were carried out in 50 μL total volume with 80 ng of total RNA and 32 pmol of each primer. First-strand synthesis was done at 48°C for 30 minutes. For CTGF amplification, PCR cycles were run at 95°C for 15 seconds, 60°C for 2 minutes, for a total of 28 cycles. For 18S rRNA amplification, PCR cycles were run at 95°C for 15 seconds, 60°C for 1 minute, for a total of 20 cycles. The PCR products were electrophoresed through a 2% agarose gel, visualized with ethidium bromide, and photographed. A similar RT-PCR procedure was carried out to monitor CTGF expression in HTS-2T and HTS-40C cells, with a total RNA of 200 ng per reaction.

Retroviral infection. The pRc/CMV-CTGF plasmid containing human CTGF cDNA was a kind gift from Dr. Gary Grotendorst (Lovelace Respiratory Research Institute, Albuquerque, NM; ref. 16, 26). For the construction of pBMN-CTGF-I-enhanced green fluorescent protein (EGFP) vector for retroviral delivery of CTGF, the human CTGF cDNA coding sequence was excised with *Eco*RI from pRc/CMV-CTGF vector and ligated into the pBMN-I-EGFP retroviral vector kindly provided by Dr. Gary Nolan with the same restriction site. Clones were sequenced to ensure correct CTGF cDNA orientation and sequence.

The pBMN-CTGF-I-EGFP vector (bicistronic) or pBMN-I-EGFP control vector were transfected into Phoenix E cells with a calcium phosphate transfection kit (Invitrogen) following a modified protocol. In brief, Phoenix cells were seeded at 1.5×10^6 cells in a 6 cm culture plate 24 hours before transfection. For transfection, 10 μg of DNA and 61 μL of 2 mol/L $CaCl_2$ were brought to 0.5 mL with double-distilled water and added dropwise to 0.5 mL of 2× HBS, while aerating with a pipette, and followed by 30-minute incubation at room temperature to form fine precipitates. To Phoenix cells in 6 cm plates in 3 mL media, 2 μL of 50 mmol/L chloroquine stock were added. Five minutes later, DNA/$CaHPO_4$ precipitates were added dropwise, followed by overnight incubation at 37°C. Medium was replaced 24 hours after transfection and plates were incubated at 32°C. Virus in the supernatant from each retrovirus-producing line was collected 48 hours after transfection and filtered (0.45 μm). Three milliliters of viral supernatant with additional 5% FBS, 5% Nu serum (BD Biosciences), 0.5 μg/mL testosterone (Sigma), 5 μg/mL insulin, and 5 μg/mL polybrene was applied immediately to C57B prostate stromal cells at 60% to 80% confluence in T25 flask. Infection was carried out at 37°C. Viral supernatant was replaced with fresh Bfs medium 24 hours after infection. Expression of retroviral construct was confirmed by counting the percentage of green fluorescent (GFP positive) C56B cells per ×100 field. Infected cultures with a >90% green fluorescent cells per field were passaged and frozen (−80°C) in 4×10^6 cells/vial aliquots for use in DRS xenografts.

3T3 cell GeneSwitch system. The GeneSwitch system (Invitrogen) was used to engineer 3T3 fibroblast cells with mifepristone (RU 486) inducible expression of a V5-His tagged CTGF protein. GeneSwitch-3T3 cells expressing the GeneSwitch regulatory protein from the pSwitch vector were purchased from Invitrogen. For the construction of pGene CTGF-V5-His vector, the human CTGF cDNA was PCR amplified from pRc/CMV-CTGF with primers 5′-CTAGGATCCGCCCGCAGTGCC-3′ (*Bam*HI) and primer 5′-TCTCTGGGGCCCTGCCATGTCTCCGTACATCTTC-3′ (*Apa*I). PCR cycles were run at 95°C for 30 seconds, 60°C for 30 seconds, and 72°C for 80 seconds for a total of 20 cycles after first incubation at 95°C for 2 minutes. The PCR reaction was incubated at 72°C for another 10 minutes for final extension. PCR products were purified with QIAquick PCR purification kit (Qiagen). After digestion with *Bam*HI and limited digestion with *Apa*I (to avoid internal *Apa*I site along CTGF cDNA sequence), the 1.1 kb CTGF insert was

gel purified and cloned in frame into the pGene/V5-His A vector (Invitrogen). Fidelity was confirmed by sequence analysis. The pGene CTGF-V5-His vector or pGene/V5-His empty vector control was transfected into GeneSwitch-3T3 cell line (Invitrogen) with FuGENE 6 transfection reagent (Roche Diagnostics Corp., Indianapolis, IN), following the protocol of the manufacturer. Stable transfected GeneSwitch-3T3 cells were selected and maintained in media (as described previously) containing 50 μg/mL of Hygromycin B and 200 μg/mL of Zeocin. Mifepristone (100 pmol/L) was used to induce CTGF-V5-His fusion protein expression. Regulated expression was confirmed by Western blot analysis of secreted proteins.

To render engineered GeneSwitch-3T3 pGene CTGF-V5-His and GeneSwitch-3T3 pGene/V5-His cells less proliferative and less tumorigenic for use in the DRS xenograft model, the cells were irradiated with increasing doses of γ-irradiation. The γ-irradiation dosage of 800 rad was chosen for DRS xenograft tumor experiments because it resulted in viable cells with a low proliferation rate and high expression of mifepristone-inducible CTGF-V5-His protein *in vitro* (Western blot, data not shown).

Western blot analysis. For V5 Western blot, conditioned medium from GeneSwitch-3T3 pGene CTGF-V5-His cells induced with 100 pmol/L mifepristone (or vehicle control) was electrophoresed through a 12% SDS-PAGE gel. Proteins were transferred onto nitrocellulose membrane (Bio-Rad Laboratories, Hercules, CA) and incubated in PBS buffer with 5% nonfat milk at 4°C overnight. Mouse anti-V_5 monoclonal antibody (Invitrogen), diluted at 1:5,000, was used as primary antibody to detect the presence of CTGF-V5-His fusion protein, and incubated for 2 hours at room temperature. Secondary antibody was biotin-conjugated sheep anti-mouse IgG (Sigma), diluted at 1:1,000, and incubated for 1 hour at room temperature. A streptavidin-horseradish peroxidase conjugate (Amersham Pharmacia Biotech UK, Ltd., Buckinghamshire, United Kingdom) diluted at 1:1,000 was incubated for 30 minutes at room temperature. Protein bands were detected by incubation with ECL+ Western blotting detection system (Amersham Biosciences) for 5 minutes at room temperature followed by exposure to Hyperfilm ECL from Amersham Pharmacia Biotech.

For CTGF Western blot, C57B CTGF and control cells were grown in Bfs to 80% confluence, then switched to serum-free M_0 media for 2 days. The media were collected and concentrated 20-fold by Amicon Ultra 4 centrifugation (5000 MWCO; Millipore, Billerica, MA). The concentrated samples were electrophoresed through a 12% SDS-PAGE gel and proteins were transferred onto Immobilon-P (Millipore). The membrane was incubated in PBS buffer with 2.5% normal donkey serum at 4°C overnight. The immunoblot protocol was the same as above, except the primary antibody was goat anti-CTGF antibody L-20 (Santa Cruz Biotechnology, Inc., Santa Cruz, CA), diluted at 1:400, and secondary antibody was biotin-conjugated donkey anti-goat antibody (Jackson ImmunoResearch Laboratories Inc., West Grove, PA), diluted at 1:40,000.

Animals and preparation of differential reactive stromal xenografts. Athymic NCr-*nu/nu* male homozygous nude mice, 6 to 8 weeks of age, were purchased from Charles River Laboratories (Wilmington, MA). All experiments were in compliance with the NIH Guide for the Care and Use of Laboratory Animals and according to the institutional guidelines of Baylor College of Medicine.

DRS xenograft tumors were generated following procedures we have published previously (2, 3, 34). Briefly, frozen aliquots of LNCaP human prostate cancer cells (16×10^6) and the engineered stromal cells—C57B-CTGF (8×10^6 cells), C57B-control (8×10^6 cells), and γ-irradiated GeneSwitch-3T3 pGene CTGF-V5-His cells (4×10^6 cells)—were thawed in a 37°C water bath for 1 to 2 minutes and washed once with 10 mL RPMI supplied with 10% serum (for LNCaP cells) or with 10 mL DMEM supplied with 10% serum (for stromal cells) in 15 mL conical tubes. The cells were pelleted at $1,400 \times g$ for 2 minutes and resuspended in 6 mL RPMI 1640 with 10% FBS. The LNCaP cells were then combined with stromal cells, mixed well, and pelleted again at $1,400 \times g$ for 2 minutes. The supernatant was aspirated to either 300 μL (for Matrigel experiments) or 200 μL [for growth factor–reduced (GFR) matrix mixture experiments] and cells were resuspended in the remaining medium. Cells were incubated on ice for 1.5 minutes and then combined with either 0.5 mL of Matrigel (Becton Dickinson, Bedford, MA) or 0.6 mL of a GFR matrix mixture composed of a 1:1 ratio of neutralized Vitrogen 100 (99.9% collagen type I; Cohesion, Palo Alto, CA) and GFR Matrigel (Becton Dickinson). In all experiments, the final volume was 800 μL. The cell and matrix mixture was drawn into a 1 mL syringe fitted with a 20-gauge needle. After switching to a 25-gauge needle, 100 μL of the cell-matrix suspension was injected s.c. in each lateral flank of adult NCr-*nu/nu* male mice.

To induce expression of CTGF-V5-His, mice with DRS xenografts composed of LNCaP cells combined with γ-irradiated GeneSwitch-3T3 pGENE CTGF-V5-His cells received mifepristone (Sigma) or vehicle control (sesame seed oil; Sigma) at 0.5 mg/kg administered as 100 μL i.p. injections at the time of tumor injection and repeated every 48 hours until tumors were harvested. This mifepristone dose was based on protocols shown previously to induce consistent gene expression *in vivo* and had no affect on xenograft tumor weight or volume (data not shown). All mifepristone experiments are in accordance with our approved Animal Use Protocols and institutional guidelines of Baylor College of Medicine.

Tumors were collected at different time points between days 10 and 21 postinoculation. For the experimental sets of LNCaP cells combined with C57B-CTGF or C57B-control cells, the tumors were photographed *in situ* for GFP expression to confirm gene expression using a fluorescent dissecting microscope. The tumors were weighed, measured in three dimensions, and fixed in 4% paraformaldehyde (neutral buffered) at 4°C overnight, washed three times in PBS, and processed for paraffin embedding. Tumors were paraffin-embedded and 5 μm sections were cut and mounted onto ProbeOn Plus slides (Fisher Scientific, Pittsburgh, PA). Sections were either stained with H&E for histologic analysis or processed for immunohistochemistry.

Immunohistochemistry. Primary antibodies were as follows: anti-mouse CD31/platelet/endothelial cell adhesion molecule 1 antibody (rat monoclonal MEC13.3; BD PharMingen, San Diego, CA); anti-V5 mouse monoclonal antibody 46-0705 (Invitrogen); rabbit anti-GFP antibody A-11122 (Molecular Probes, Eugene, OR); goat anti-CTGF antibody L-20 (Santa Cruz). Secondary antibodies were as follows: biotin-conjugated goat anti-rat IgG (BD PharMingen) for CD31, biotin-conjugated Universal Secondary (Invitrogen) for V5, biotin-conjugated goat anti-rabbit IgG B8895 (Sigma) for GFP, and biotin-conjugated donkey anti-goat antibody (Jackson ImmunoResearch Laboratories). Specificity of each primary antibody has been evaluated previously (refs. 2, 3, 34; and unpublished data).

Immunostaining was done with the MicroProbe Staining System (Fisher Scientific) following our protocol published previously (2, 3, 34). Reagents formulated for use with capillary action systems were purchased from Open Biosystems (Huntsville, AL) and used according to the protocol of the manufacturer. In brief, tissues were deparaffinized using Auto Dewaxer and cleared with Auto Alcohol. Brigati's iodine and Auto Prep were used to improve tissue antigenicity. Antigen retrieval were used in CD31, V5, and CTGF staining. For CD31 staining, tissues were incubated in 0.1% trypsin (Zymed, South San Francisco, CA) for 10 minutes at 37°C; for V5 and CTGF staining, tissues were subjected to high-temperature-steamer treatment in 10 mmol/L sodium citrate buffer (pH 6.0) for 20 minutes. Goat anti-mouse Fab fragment (Jackson ImmunoResearch Laboratories) 1:65 was used for 30 minutes at 37°C for blocking before anti-V5 immunostaining. Sections were then incubated in protein blocker (for V5, CD31, and GFP) or 5% normal donkey serum in universal buffer (for CTGF). Primary antibodies were diluted and used under the following conditions: V5 (1:200), CD31 (1:50), GFP (1:200) in primary antibody diluent, and CTGF (1:100) in 5% normal donkey serum overnight at 4°C. Secondary antibodies were diluted and used under following conditions: biotin-conjugated universal secondary antibody for 4 minutes at 50°C; biotin-conjugated goat anti-rat IgG 1:100; biotin-conjugated goat anti-rabbit IgG 1:500; and biotin-conjugated donkey anti-goat antibody 1:200 for 45 minutes at 37°C. Tissues were treated with Auto Blocker to inhibit endogenous peroxidase activity. For detection, sections were incubated in RTU VectaStain Elite ABC reagent (Vector

Laboratories, Burlingame, CA) and then incubated in stable diaminobenzidine tetrahydrochloride twice for 3 minutes each at 50°C. Tissues were counterstained with Auto Hematoxylin for 30 seconds.

Microvessel density analysis. Analysis was done according to standard procedures we have published previously with DRS tumors (2, 3, 34). Tissue sections were stained for CD31 as described above. Sections were scanned at ×100, and five random areas per tumor section were selected. Vessels in these fields were counted (at ×400) by an observer blinded to experimental conditions. The average vessel count was determined for each specimen.

Statistical analysis. Tumors from each condition were analyzed, and average tumor weight and average microvessel counts were compared with these values from their matching control tumors for statistical relevance using the unpaired *t* test. Statistical analyses used GraphPad Prism for Macintosh version 3.0 (GraphPad Software, San Diego, CA). $P < 0.05$ was considered statistically significant.

Results

Differential expression of connective tissue growth factor in tumor-promoting human prostate stromal cell lines. Our previous studies using the DRS xenograft model showed that several human prostate stromal cell lines differentially promote LNCaP prostate cancer cell tumorigenesis (2). Stromal cell–promoted tumors exhibited a significantly elevated rate of angiogenesis and this was TGF-β1 regulated (2, 3). Notably, the HTS-40C and the HTS-2T human prostate stromal cell lines exhibited opposing effects. In two-way DRS xenografts constructed of cancer cells and stromal cells in the absence of extracellular matrix (Matrigel), the HTS-40C/LNCaP combinations resulted in a 65% tumor incidence, whereas HTS-2T/LNCaP combinations were nontumorigenic (0% tumor incidence; ref. 2). To address potential mechanisms, gene expression profiles in HTS-40C and HTS-2T stromal cells were compared using cDNA microarray analyses. This analysis showed that 12 previously characterized genes were elevated by 3- to 31-fold in the protumorigenic HTS-40C stromal cell line compared with HTS-2T. These genes are listed in Table 1. Expression of several of these genes is associated with reactive stroma that forms at sites of wound repair, microbial invasion, or carcinoma as we have reported previously (1, 32, 35). Of these, CTGF is a known inducer of angiogenesis (36), is TGF-β1 regulated in stromal cells (18, 37–39), and has been reported to directly enhance TGF-β1 receptor-ligand binding (40). Our microarray data suggested that CTGF message was 4.5-fold higher in HTS-40C cells compared with HTS-2T cells. Further analysis confirmed this with RT-PCR and showed that CTGF message expression was severalfold higher in HTS-40C cells relative to HTS-2T cells as shown in Fig. 1*A*.

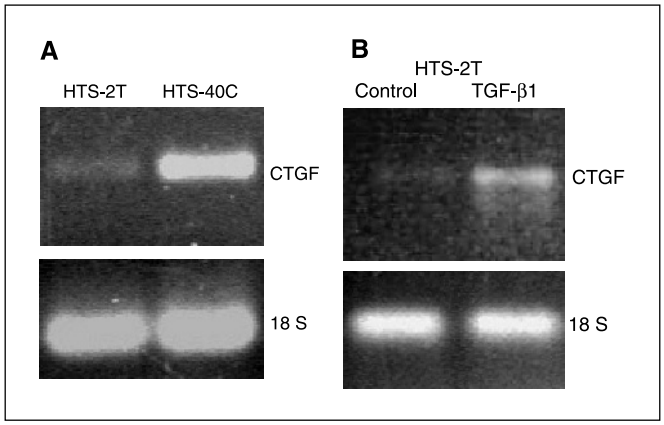

Figure 1. Expression of CTGF message in different prostate stromal cell lines. *A,* RT-PCR–amplified products from HTS-40C cells compared with HTS-2T cells. *B,* HTS-2T cells exposed to TGF-β1 (100 pmol/L) or vehicle control for 24 hours. In both cases, 18S rRNA amplifications were used as loading control.

Although the HTS-2T stromal cell line did not support LNCaP tumorigenesis in matrix-free conditions (two-way tumors), HTS-2T cells did promote LNCaP tumors (incidence, rate of tumorigenesis, and angiogenesis) when combined with Matrigel matrix in three-way DRS xenografts that are constructed with cancer cells, stromal cells, and Matrigel matrix (2, 3). Matrigel matrix is high in TGF-β1 and we have reported that inhibiting TGF-β1 activity in Matrigel lowers the rate of tumorigenesis and angiogenesis in three-way DRS tumors (3). Accordingly, we next determined whether TGF-β1 could induce CTGF expression in human prostate HTS-2T stromal cells. As shown in Fig. 1*B*, HTS-2T cells in control conditions exhibited low expression, whereas HTS-2T cultures exposed to TGF-β1 (100 pmol/L, 24 hours) exhibited elevated CTGF message expression. This is in agreement with previous reports showing TGF-β1 regulation of CTGF expression in other stromal cell lines (15, 19).

Table 1. Genes up-regulated in the HTS-40C cells compared with HTS-2T cells

40C/2T	Gene	UniGene no.	Accession no.	Gene description
31.333	*PLOD2*	Hs.477866	U84573	Procollagen-lysine, 2-oxoglutarate 5-dioxygenase 2
10.800	*TRAP1*	Hs.30345	U12595	Tumor necrosis factor receptor–associated protein 1
7.666	*TP53BP2*	Hs.523968	AI123916	Tumor protein p53-binding protein, 2
5.847	*ARF3*	Hs.119177	M74493	ADP ribosylation factor 3
4.899	*CFH*	Hs.363396	M12383	Complement protein H
4.637	*FMO*	Hs.132821*	AL021026	Flavin-containing monooxygenase
4.466	*CTGF*	Hs.75511	U14750	Connective tissue growth factor
3.841	*THBS1*	Hs.164226	NM_003246	Thrombospondin 1
3.574	*BRAP*	Hs.530940	AF035950	BRCA1-associated protein
3.152	*ADH1A*	Hs.368549	NM_000667	Alcohol dehydrogenase 1A (class I), α polypeptide
3.130	*PTSG1*	Hs.201978	U63846	Prostaglandin-endoperoxide synthase 1 (prostaglandin G/H synthase and cyclooxygenase)
3.083	*PTX3*	Hs.546280	M31166	Pentraxin-related gene, rapidly induced by interleukin-1β

*Retired UniGene number without concise replacement.

Expression of connective tissue growth factor in prostate stromal cells promotes angiogenesis and LNCaP tumorigenesis. A construct containing the full-length human CTGF cDNA (kindly provided by Dr. Gary Grotendorst) was used to construct a bicistronic retroviral vector (pBMN-CTGF-I-EGFP) containing CTGF followed by an IRES and EGFP for detection of expression. Either vector control (pBMN-I-EGFP) or the CTGF-containing retrovirus preparations were used to infect the mouse prostate stromal cell line (C57B) and cells were analyzed for fluorescence 48 hours later as described in Materials and Methods. Figure 2*A* shows infected and EGFP-expressing C57B stromal cells before use in the DRS xenograft. C57B cells routinely exhibited a 90% infectivity rate or higher (data not shown). Western blot analysis showed overexpression of the mature form of CTGF (~38 kDa) in the experimental cell conditioned medium and low endogenous levels in the control infected cultures (Fig. 2*B*). Shorter fragments were also observed (Fig. 2*B*, *band A* and *band B*), which have been reported in the conditioned media of CTFG-secreting cells by others (41).

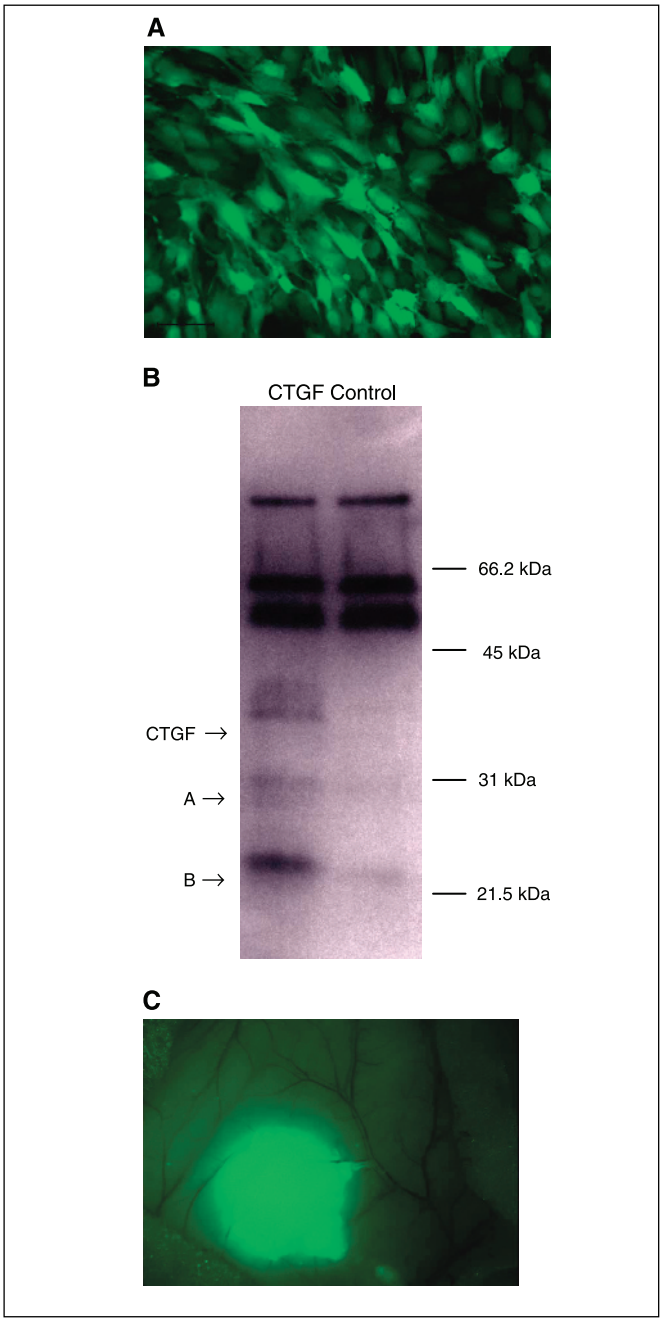

Figure 2. Transgene expression in retroviral-infected C57B prostate stromal cells and DRS tumors. *A,* GFP fluorescence of retroviral (pBMN-CTGF-I-EGFP) infected C57B cells *in vitro*. *Bar*, 100 μm. *B,* Western blot analysis of CTGF protein in conditioned media of pBMN-CTGF-I-EGFP–infected C57B cells (*CTGF*) compared with pBMN-I-EGFP control vector infected cells (*Control*). *C,* GFP fluorescence of tumors *in situ*. An incision was made in the skin immediately adjacent to the s.c. tumor. The skin flap was turned back and photographed with a fluorescent dissecting microscope.

To evaluate the effects of CTGF expression from prostate stromal cells in three-way LNCaP tumors in nude mice, we inoculated cell combinations in either complete Matrigel or a modified matrix composed of a 1:1 mix of GFR Matrigel together with neutralized Vitrogen 100 collagen type I (GFR Matrigel/Vitrogen) to reduce bioactive factors in the matrix component. S.c. three-way DRS xenograft tumors were constructed in male nude mice using 2×10^6 LNCaP cells, and 1×10^6 control C57B (EGFP-expressing vector only) or CTGF-expressing C57B prostate stromal cells and the different Matrigel matrix preparations as described in Materials and Methods. Tumors were harvested at day 13 postinoculation because our previous studies have shown that day 10 to day 14 postinoculation is the optimal time frame to assess initial rate of angiogenesis and tumorigenesis (2, 3, 34). It should be noted that control or CTGF-transduced C57B cells inoculated alone or with matrix were nontumorigenic (data not shown) similar to our previous report (2). As shown in Fig. 2*C*, tumors were fluorescent *in situ* before removal. This confirmed transgene expression and viability of the engineered C57B stromal cells in the tumor xenograft.

Tumors exhibited a typical arrangement of LNCaP carcinoma cell clusters, surrounded by stromal cells, matrix, and vessels as shown in Fig. 3*A* and *B*, similar to what we have reported previously (2). There were no particular differences in histology or ratio of carcinoma to stromal cells in experimental tumors compared with control tumors. Prostate stromal cells engineered with the CTGF transgene in tumors were positive for both EGFP (Fig. 3*C*) and CTGF (Fig. 3*D*) proteins, and were immediately adjacent to clusters of LNCaP carcinoma cells. Immunostaining for CD31 as an endothelial marker showed an obvious difference in vessels. The density of CD31-positive microvessels in CTGF-expressing xenografts (Fig. 3*F*) seemed higher compared with control xenografts (Fig. 3*E*). Microvessel counts confirmed this. In complete Matrigel conditions, LNCaP xenograft tumors constructed with CTGF-expressing prostate stromal cells exhibited a microvessel density of 10.60 ± 1.35 compared with 6.16 ± 1.60 in vector-only control tumors ($n = 25$ fields, five tumors each, mean $\pm$ SE, $P < 0.05$; Fig. 4*A*). This represented a 72% increase in vessel density in the stromal CTGF-expressing tumors. The increase in vessel density correlated with elevated tumor mass. The mean wet weight of stromal CTGF-expressing LNCaP tumors was 24.42 ± 0.76 mg compared with 18.08 ± 1.54 mg ($n = 5$, mean $\pm$ SE, $P < 0.01$; Fig. 4*B*) in control tumors, indicating that stromal CTGF expression produced a 35% increase in tumor mass when xenografts are constructed in complete Matrigel conditions.

Significant differences in angiogenesis were even more pronounced in the low growth factor–modified matrix (GFR Matrigel/Vitrogen 100) conditions. CTGF-expressing tumors exhibited an average microvessel density of 10.10 ± 1.73

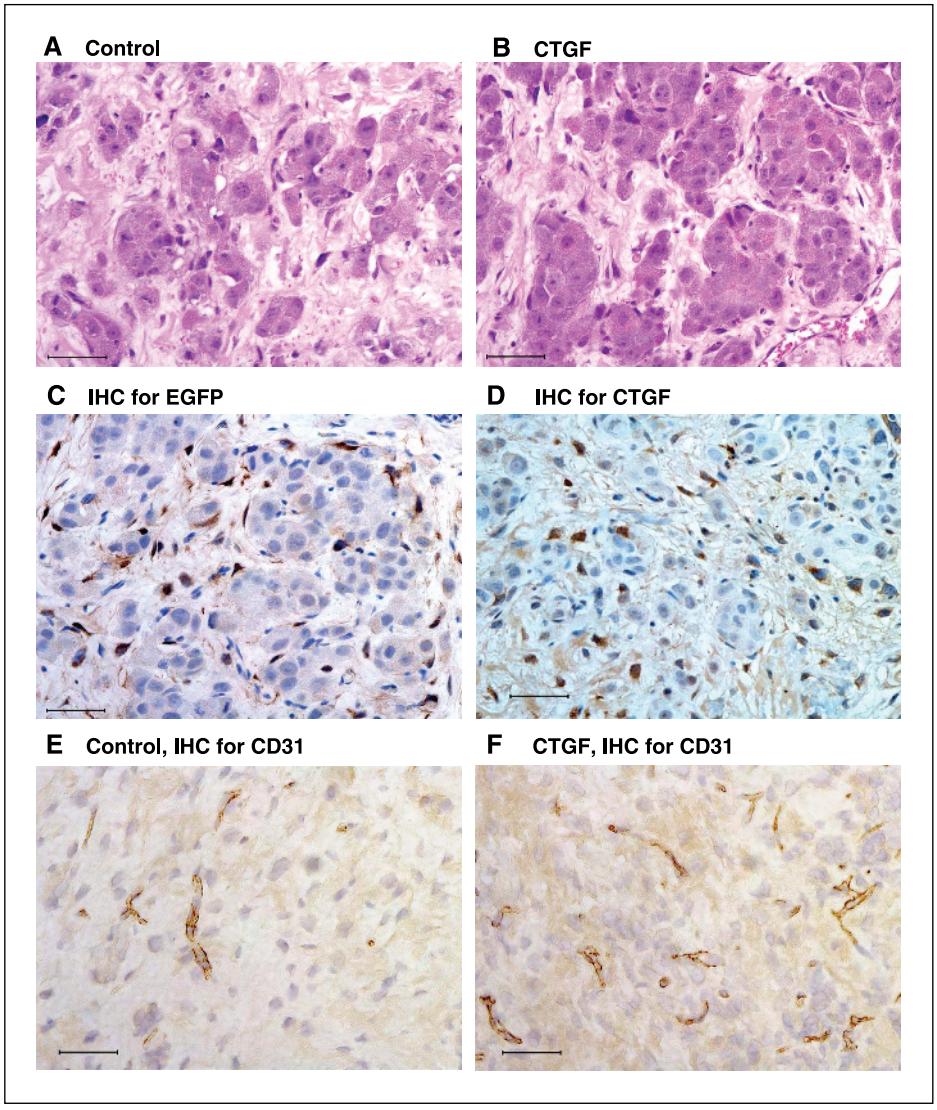

Figure 3. Histologic analysis of three-way LNCaP DRS xenograft tumors constructed with control or CTGF-expressing prostate stromal cells. *A* and *B,* the histology of DRS tumors generated from LNCaP cells combined with control C57B cells (*A*) or CTGF-expressing C57B cells (*B*). *C,* immunohistochemistry of EGFP expression in tumor stromal cells. *D,* immunohistochemistry of CTGF expression in tumor stromal cells. *E,* immunohistochemistry of CD31 expression in vessels from tumors constructed with control stromal cells. *F,* immunohistochemistry of CD31 expression in vessels of tumors constructed with CTGF-expressing stromal cells. *Bar*, 50 μm.

compared with 4.70 ± 1.00 in control tumors, representing a 115% increase over control (n = 30, from six tumors in each condition, mean ± SE, P < 0.01; Fig. 4*C*). The stromal CTGF-expressing LNCaP tumors constructed in the GFR-modified matrix showed an average wet weight of 17.58 ± 0.60 mg compared with 12.97 ± 0.71 mg in control tumors (n = 18 in the CTGF experimental and n = 17 in the control, mean ± SE, P < 0.0001; Fig. 4*D*), representing a 36% increase in tumor mass.

Regulated expression of CTGF-V5-His in 3T3 fibroblasts promotes LNCaP tumorigenesis. To confirm and extend the findings with retroviral transduced C57B cells, the GeneSwitch System (Invitrogen) was used to engineer 3T3 stromal cell lines with mifepristone-regulated expression of an epitope-tagged CTGF-V5-His (fusion protein). Cultures at 80% to 100% confluence were induced with 100 pmol/L mifepristone for 24 to 48 hours. Western blot analysis for the V5 epitope showed an inducible 41 kDa CTGF-V5-His band in the conditioned media (Fig. 5*A*). DRS xenograft tumors were generated in nude mice using 2 × 10^6 LNCaP cells combined with γ-irradiated 5 × 10^5 GeneSwitch-3T3 pGene CTGF-V5-His cells and complete Matrigel (three-way DRS xenograft conditions). Irradiated engineered 3T3 cells (800 rad) were used because these cells remain viable, exhibit regulated transgene expression, and have a low proliferative rate relative to wild-type NIH 3T3 cells. Mice were given mifepristone or vehicle i.p. every 48 hours as described in Materials and Methods. Our previous studies have shown that this protocol of mifepristone treatment has no ill effect on nude mice and does not affect control tumor biology (2, 34). Resulting tumors were harvested 10 days postinoculation. Immunohistochemistry showed tightly regulated CTFG-V5-His protein expression *in vivo* (Fig. 5*B*). No expression was noted in tumors derived from vehicle control-treated animals (Fig. 5*C*). Tumors exhibited a typical carcinoma phenotype similar to the LNCaP/C57B combinations, although the tumors were considerably more heterogeneous with more focal nodules of carcinoma and other areas that seemed to have little carcinoma growth. There was, however, no apparent difference in histopathology noted between vehicle control and mifepristone-treated animals. LNCaP DRS tumors from mifepristone-treated animals exhibited a 25% average increase in wet weight as shown in Fig. 5*D*. The mean weight of control tumors was 17.91 ± 1.04 mg, whereas tumors from mifepristone-treated animals averaged 22.41 ± 1.76 mg (P < 0.05,

n = 12 tumors each). The tumors exhibited a very heterogeneous density of microvessels, as might be expected, due to the nodular and heterogeneous histopathology. This was obvious at low-power observation (data not shown). The heterogeneous nature of the vessel density patterns in these tumors was not compatible with the microvessel-counting protocol (see Materials and Methods) as the accuracy of this method is dependent on uniform vessel distribution. Accordingly, no attempt was made to quantitate microvessel density in these tumors as these data would not be accurate.

Discussion

To date, no effective approach exists to manipulate overexpression of a transgene in the stromal compartment in a tissue-specific manner *in situ*. Accordingly, we have used the DRS xenograft tumor approach to test the biological consequences of differential transgene expression in the reactive stroma compartment of an experimental human tumor in a nude mouse host. Our previous studies have shown that use of different human prostate stromal cell lines result in vast differences in LNCaP tumorigenesis *in vivo* (2). Furthermore, we have shown that the endogenous TGF-β1 activity in complete Matrigel is responsible for this difference in both angiogenesis and tumorigenesis (3). Our current study shows that CTGF may mediate TGF-β1 actions in the prostate stromal cells. Expression of a CTGF transgene in the reactive stromal compartment of LNCaP DRS xenograft tumors resulted in enhanced tumorigenesis that was correlated with a more rapid rate of angiogenesis. We conclude from these data that CTGF may be an important regulator of tumor-reactive stroma and angiogenesis.

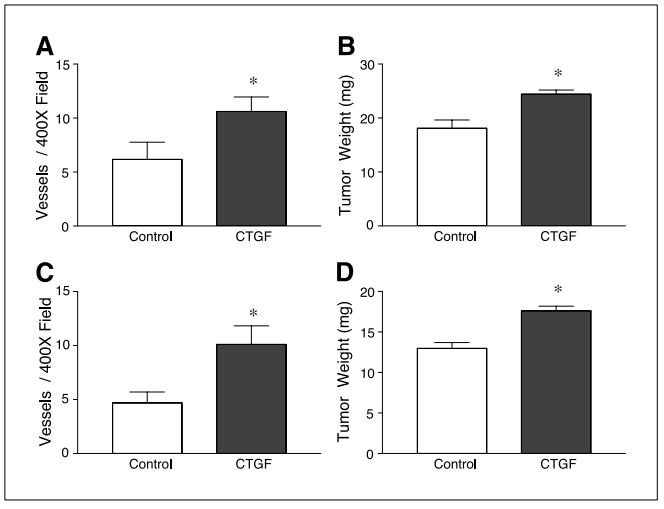

Figure 4. Stromal expression of CTGF stimulates microvessel density and tumor weight in three-way LNCaP DRS tumors constructed in different matrix preparations. *A* and *B,* microvessel densities and tumor weights were compared between the LNCaP tumors generated in the presence of C57B prostate stromal cells engineered to express CTGF (*CTGF*) or vector control stromal cells (*Control*), in complete BD Matrigel conditions at day 13 postinoculation. *A,* microvessel density, as assessed by CD31-positive structures, counted by a blinded observer (n = 25 fields, five tumors for each group). *Statistically significant increase in tumor microvessel density for DRS tumors generated in the presence of stromal cells expressing CTGF ($P < 0.05$). *B,* tumor wet weight (n = 5). *Statistically significant increase in wet weights of CTGF-expressing tumors when compared with control tumors ($P < 0.01$). *C* and *D,* microvessel densities and tumor weight were compared between the LNCaP tumors generated in the presence of C57B cells engineered to express CTGF (*CTGF*) or vector control C57B stromal cells (*Control*), in the low growth factor modified matrix (GFR Matrigel/Vitrogen 100) conditions at day 13 postinoculation. *C,* microvessel density, as assessed by CD31-positive structures, counted by a blinded observer (n = 30 fields, six tumors for each group). *Statistically significant increase in tumor microvessel density for DRS tumors generated in the presence of stromal cells expressing CTGF ($P < 0.01$). *D,* tumor wet weight (n = 17 in the control and n = 18 in the CTGF experimental). *Statistically significant increase in wet weights of CTGF expression tumors when compared with control tumors ($P < 0.0001$).

Our studies and others have suggested that reactive stroma in carcinomas is an important process associated with early events in tumorigenesis, including the formation of a wound repair type of matrix and enhanced angiogenesis (1–3, 32). Reactive stroma is remarkably similar in most carcinomas. Typically, carcinoma-associated reactive stroma is composed of activated fibroblasts and myofibroblasts, characteristic of a wound repair–type stroma (1, 32, 35). A key feature of wound repair stroma is rapid and elevated angiogenesis. In wounding, platelet-released TGF-β1 and platelet-derived growth factor function to regulate stromal cell phenotype changes and to stimulate stromal cell migration, matrix production, and angiogenesis. TGF-β1 is overexpressed by cancer epithelial cells in most carcinomas, including prostate cancer (32, 35). Moreover, CTGF is TGF-β1 regulated in a diverse set of cell types, including human prostate stromal cells as reported here (15–19). In addition, CTGF has been shown to stimulate a wound repair type of stroma in several key studies and has been shown to mediate, in part, TGF-β1–induced matrix remodeling (20). Hence, it is important to determine whether CTGF mediates a TGF-β1–stimulated reactive stroma response in cancer and whether this reactive stroma is tumor promoting. Data reported here address this question directly and suggests that TGF-β1 stimulated CTGF expression in carcinoma-associated reactive stroma, promotes angiogenesis, and results in enhanced tumorigenesis.

It is becoming clearer that the classic regulators of wound repair play an important role in carcinoma-reactive stroma and CTGF biology. For example, both fibroblast growth factor-2 (FGF-2) and vascular endothelial growth factor have been reported to stimulate CTGF expression (25, 42). FGF-2 expression is also TGF-β1 regulated in fibroblasts from the prostate gland and other tissues (43, 44). Hypoxia will induce CTGF expression via a hypoxia-inducible factor-1α pathway (45). In addition, thrombin and plasma clotting actor VIIa also induce CTGF expression (46). Accordingly, several factors and conditions associated with wound repair are known to affect CTGF expression and many of these factors and conditions are likely to play a role in tumor-associated reactive stroma.

The specific mechanisms of how CTGF or closely related family members directly affect reactive stromal cells in the tumor microenvironment is not fully understood. It is known that both CTGF and Cyr61 promote fibroblast adhesion through integrin α6β1 and that this process requires cell surface heparan sulfate proteoglycans (47). Cry61 and CTGF also stimulated migration and proliferation of fibroblasts, as well as endothelial cells (24, 48). In addition, CTGF also affects matrix production and remodeling. For example, CTGF was shown to stimulate fibronectin expression via a p42/44 mitogen-activated protein kinase and phosphoinositide 3 kinase/protein kinase B pathway (49). It will be important to dissect key CTGF signaling pathways in reactive stroma associated with tumors. Key components of these mechanisms may be useful as targets of therapeutic approaches directed at the tumor microenvironment.

The DRS model described in this study brings the opportunity to use highly efficient gene delivery and stable gene integration

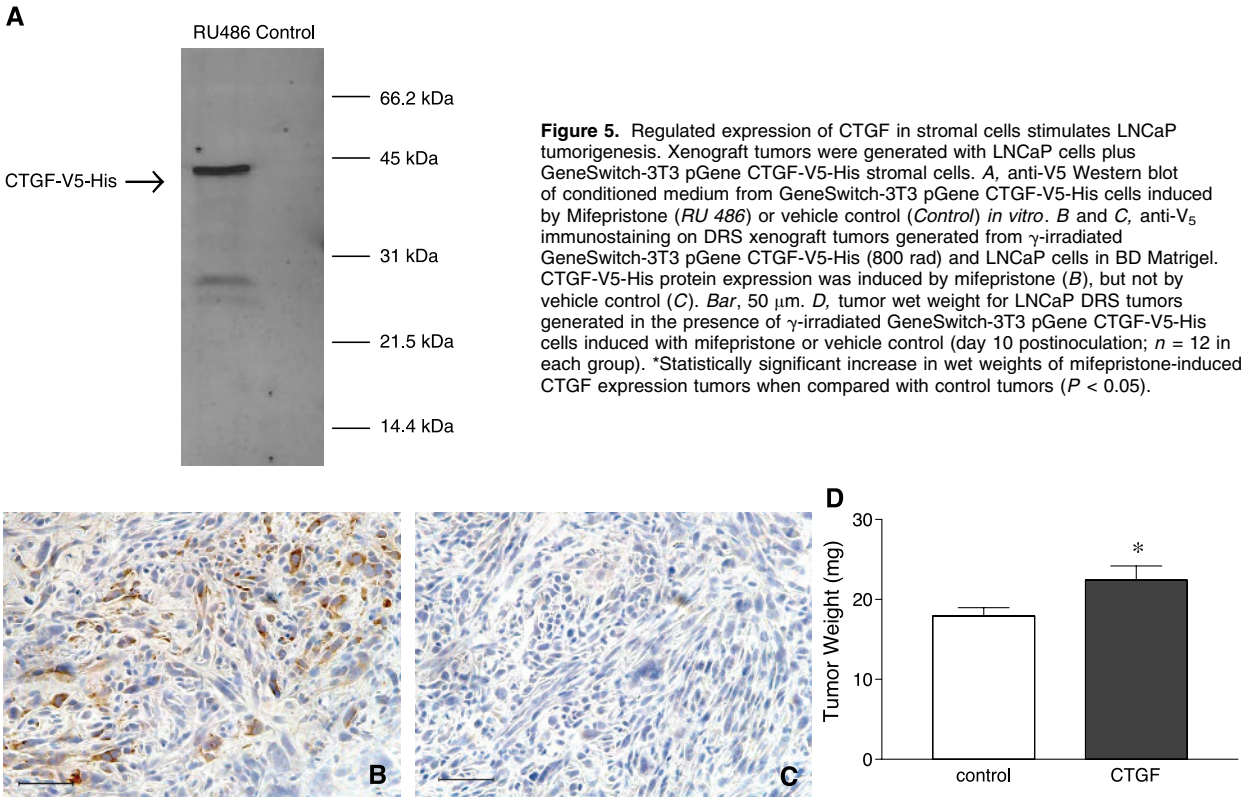

Figure 5. Regulated expression of CTGF in stromal cells stimulates LNCaP tumorigenesis. Xenograft tumors were generated with LNCaP cells plus GeneSwitch-3T3 pGene CTGF-V5-His stromal cells. *A,* anti-V5 Western blot of conditioned medium from GeneSwitch-3T3 pGene CTGF-V5-His cells induced by Mifepristone (*RU 486*) or vehicle control (*Control*) *in vitro*. *B* and *C,* anti-V_5 immunostaining on DRS xenograft tumors generated from γ-irradiated GeneSwitch-3T3 pGene CTGF-V5-His (800 rad) and LNCaP cells in BD Matrigel. CTGF-V5-His protein expression was induced by mifepristone (*B*), but not by vehicle control (*C*). *Bar*, 50 μm. *D,* tumor wet weight for LNCaP DRS tumors generated in the presence of γ-irradiated GeneSwitch-3T3 pGene CTGF-V5-His cells induced with mifepristone or vehicle control (day 10 postinoculation; $n = 12$ in each group). *Statistically significant increase in wet weights of mifepristone-induced CTGF expression tumors when compared with control tumors ($P < 0.05$).

of retroviral-infected mouse prostate stromal cell lines to study the roles of epithelial cell-stromal cell interactions in carcinoma tumorigenesis and progression. Accordingly, the DRS model has allowed for the ability to dissect out the roles of individual growth factors in the reactive stroma compartment of a tumor. Data reported here represent the first study to show that expression of CTGF in the tumor microenvironment stromal cells of an experimental epithelial cancer functions to stimulate angiogenesis and tumor growth.

Emerging data supports the concept that the reactive stromal tumor microenvironment functions to affect the rate of tumorigenesis in most epithelial carcinomas studied to date. Accordingly, it is likely that the biological components and specific mechanisms of reactive stroma can be used both as prognostic indicators and as targets of therapeutics. This study shows that CTFG is a TGF-β1–regulated and stromal-expressed factor that promotes tumorigenesis and is, therefore, a theoretical target for therapeutics focusing on tumor-associated reactive stroma biology.

Acknowledgments

Received 5/17/2005; revised 7/5/2005; accepted 7/22/2005.

Grant support: NIH grants RO1-DK45909, RO1-CA58093, Specialized Programs of Research Excellence CA58204, UO1-CA84296, and Department of Defense Prostate Cancer Research Program Award #W81XWH-04-1-0189.

The costs of publication of this article were defrayed in part by the payment of page charges. This article must therefore be hereby marked *advertisement* in accordance with 18 U.S.C. Section 1734 solely to indicate this fact.

We thank Dr. Michael Ittmann and Dr. Mustafa Ozen for conducting the human cDNA microarray analysis, Liz Hopkins for histologic preparation of tissue, Dr. Gary Grotendorst for providing human CTGF cDNA, and Dr. Gary Nolan for providing the pBMN-I-EGFP vector.

References

1. Tuxhorn JA, Ayala GE, Smith MJ, Smith VC, Dang TD, Rowley DR. Reactive stroma in human prostate cancer: induction of myofibroblast phenotype and extracellular matrix remodeling. Clin Cancer Res 2002;8:2912–23.
2. Tuxhorn JA, McAlhany SJ, Dang TD, Ayala GE, Rowley DR. Stromal cells promote angiogenesis and growth of human prostate tumors in a differential reactive stroma (DRS) xenograft model. Cancer Res 2002;62:3298–307.
3. Tuxhorn JA, McAlhany SJ, Yang F, Dang TD, Rowley DR. Inhibition of transforming growth factor-β activity decreases angiogenesis in a human prostate cancer-reactive stroma xenograft model. Cancer Res 2002;62:6021–5.
4. Franklin TJ. Therapeutic approaches to organ fibrosis. Int J Biochem Cell Biol 1997;29:79–89.
5. Crean JK, Lappin D, Godson C, Brady HR. Connective tissue growth factor: an attractive therapeutic target in fibrotic renal disease. Expert Opin Ther Targets 2001;5:519–30.
6. Ihn H. Pathogenesis of fibrosis: role of TGF-β and CTGF. Curr Opin Rheumatol 2002;14:681–5.
7. Brigstock DR. The connective tissue growth factor/cysteine-rich 61/nephroblastoma overexpressed (CCN) family. Endocr Rev 1999;20:189–206.
8. Lau LF, Lam SC. The CCN family of angiogenic regulators: the integrin connection. Exp Cell Res 1999;248:44–57.
9. Grotendorst GR, Lau LF, Perbal B. CCN proteins are distinct from and should not be considered members of the insulin-like growth factor-binding protein superfamily. Endocrinology 2000;141:2254–6.
10. Bradham DM, Igarashi A, Potter RL, Grotendorst GR. Connective tissue growth factor: a cysteine-rich mitogen secreted by human vascular endothelial cells is related to the SRC-induced immediate early gene product CEF-10. J Cell Biol 1991;114:1285–94.
11. Ryseck RP, Macdonald-Bravo H, Mattei MG, Bravo R. Structure, mapping, and expression of fisp-12, a growth factor-inducible gene encoding a secreted cysteine-rich protein. Cell Growth Differ 1991;2:225–33.
12. O'Brien TP, Yang GP, Sanders L, Lau LF. Expression of cyr61, a growth factor-inducible immediate-early gene. Mol Cell Biol 1990;10:3569–77.
13. Martinerie C, Viegas-Pequignot E, Guenard I, et al.

Physical mapping of human loci homologous to the chicken nov proto-oncogene. Oncogene 1992;7:2529–34.
14. Pennica D, Swanson TA, Welsh JW, et al. *WISP* genes are members of the connective tissue growth factor family that are up-regulated in wnt-1-transformed cells and aberrantly expressed in human colon tumors. Proc Natl Acad Sci U S A 1998;95:14717–22.
15. Igarashi A, Okochi H, Bradham DM, Grotendorst GR. Regulation of connective tissue growth factor gene expression in human skin fibroblasts and during wound repair. Mol Biol Cell 1993;4:637–45.
16. Frazier K, Williams S, Kothapalli D, Klapper H, Grotendorst GR. Stimulation of fibroblast cell growth, matrix production, and granulation tissue formation by connective tissue growth factor. J Invest Dermatol 1996; 107:404–11.
17. Grotendorst GR, Okochi H, Hayashi N. A novel transforming growth factor β response element controls the expression of the connective tissue growth factor gene. Cell Growth Differ 1996;7:469–80.
18. Chen MM, Lam A, Abraham JA, Schreiner GF, Joly AH. CTGF expression is induced by TGF-β in cardiac fibroblasts and cardiac myocytes: a potential role in heart fibrosis. J Mol Cell Cardiol 2000;32:1805–19.
19. Untergasser G, Gander R, Lilg C, Lepperdinger G, Plas E, Berger P. Profiling molecular targets of TGF-β1 in prostate fibroblast-to-myofibroblast transdifferentiation. Mech Ageing Dev 2005;126:59–69.
20. Duncan MR, Frazier KS, Abramson S, et al. Connective tissue growth factor mediates transforming growth factor β-induced collagen synthesis: down-regulation by cAMP. FASEB J 1999;13:1774–86.
21. Chen Y, Abraham DJ, Shi-Wen X, Black CM, Lyons KM, Leask A. CCN2 (connective tissue growth factor) promotes fibroblast adhesion to fibronectin. Mol Biol Cell 2004;15:5635–46.
22. Fan WH, Pech M, Karnovsky MJ. Connective tissue growth factor (CTGF) stimulates vascular smooth muscle cell growth and migration *in vitro*. Eur J Cell Biol 2000;79:915–23.
23. Shimo T, Nakanishi T, Nishida T, et al. Connective tissue growth factor induces the proliferation, migration, and tube formation of vascular endothelial cells *in vitro*, and angiogenesis *in vivo*. J Biochem (Tokyo) 1999;126:137–45.
24. Babic AM, Chen CC, Lau LF. Fisp12/mouse connective tissue growth factor mediates endothelial cell adhesion and migration through integrin αvβ3, promotes endothelial cell survival, and induces angiogenesis *in vivo*. Mol Cell Biol 1999;19:2958–66.
25. Brigstock DR. Regulation of angiogenesis and endothelial cell function by connective tissue growth factor (CTGF) and cysteine-rich 61 (CYR61). Angiogenesis 2002;5:153–65.
26. Frazier KS, Grotendorst GR. Expression of connective tissue growth factor mRNA in the fibrous stroma of mammary tumors. Int J Biochem Cell Biol 1997;29:153–61.
27. Wenger C, Ellenrieder V, Alber B, et al. Expression and differential regulation of connective tissue growth factor in pancreatic cancer cells. Oncogene 1999;18:1073–80.
28. Koliopanos A, Friess H, di Mola FF, et al. Connective tissue growth factor gene expression alters tumor progression in esophageal cancer. World J Surg 2002; 26:420–7.
29. Kasaragod AB, Lucia MS, Cabirac G, Grotendorst GR, Stenmark KR. Connective tissue growth factor expression in pediatric myofibroblastic tumors. Pediatr Dev Pathol 2001;4:37–45.
30. Shakunaga T, Ozaki T, Ohara N, et al. Expression of connective tissue growth factor in cartilaginous tumors. Cancer 2000;89:1466–73.
31. Blom IE, Goldschmeding R, Leask A. Gene regulation of connective tissue growth factor: new targets for antifibrotic therapy? Matrix Biol 2002;21:473–82.
32. Tuxhorn JA, Ayala GE, Rowley DR. Reactive stroma in prostate cancer progression. J Urol 2001;166:2472–83.
33. Polnaszek N, Kwabi-Addo B, Peterson LE, et al. Fibroblast growth factor 2 promotes tumor progression in an autochthonous mouse model of prostate cancer. Cancer Res 2003;63:5754–60.
34. McAlhany SJ, Ressler SJ, Larsen M, et al. Promotion of angiogenesis by ps20 in the differential reactive stroma prostate cancer xenograft model. Cancer Res 2003;63: 5859–65.
35. Rowley DR. What might a stromal response mean to prostate cancer progression? Cancer Metastasis Rev 1998;17:411–9.
36. Shimo T, Nakanishi T, Nishida T, et al. Involvement of CTGF, a hypertrophic chondrocyte-specific gene product, in tumor angiogenesis. Oncology 2001;61:315–22.
37. Grotendorst GR. Connective tissue growth factor: a mediator of TGF-β action on fibroblasts. Cytokine Growth Factor Rev 1997;8:171–9.
38. Harlow CR, Davidson L, Burns KH, Yan C, Matzuk MM, Hillier SG. FSH and TGF-β superfamily members regulate granulosa cell connective tissue growth factor gene expression *in vitro* and *in vivo*. Endocrinology 2002; 143:3316–25.
39. Kothapalli D, Hayashi N, Grotendorst GR. Inhibition of TGF-β-stimulated *CTGF* gene expression and anchorage-independent growth by cAMP identifies a CTGF-dependent restriction point in the cell cycle. FASEB J 1998;12:1151–61.
40. Abreu JG, Ketpura NI, Reversade B, De Robertis EM. Connective-tissue growth factor (CTGF) modulates cell signalling by BMP and TGF-β. Nat Cell Biol 2002;4:599–604.
41. Boes M, Dake BL, Booth BA, et al. Connective tissue growth factor (IGFBP-rP2) expression and regulation in cultured bovine endothelial cells. Endocrinology 1999; 140:1575–80.
42. Suzuma K, Naruse K, Suzuma I, et al. Vascular endothelial growth factor induces expression of connective tissue growth factor via KDR, Flt1, and phosphatidylinositol 3-kinase-akt-dependent pathways in retinal vascular cells. J Biol Chem 2000;275:40725–31.
43. Story MT, Hopp KA, Meier DA, Begun FP, Lawson RK. Influence of transforming growth factor β1 and other growth factors on basic fibroblast growth factor level and proliferation of cultured human prostate-derived fibroblasts. Prostate 1993;22:183–97.
44. Song QH, Klepeis VE, Nugent MA, Trinkaus-Randall V. TGF-β1 regulates TGF-β1 and FGF-2 mRNA expression during fibroblast wound healing. Mol Pathol 2002; 55:164–76.
45. Higgins DF, Biju MP, Akai Y, Wutz A, Johnson RS, Haase VH. Hypoxic induction of CTGF is directly mediated by Hif-1. Am J Physiol Renal Physiol 2004; 287:1223–32.
46. Pendurthi UR, Allen KE, Ezban M, Rao LV. Factor VIIa and thrombin induce the expression of Cyr61 and connective tissue growth factor, extracellular matrix signaling proteins that could act as possible downstream mediators in factor VIIa x tissue factor-induced signal transduction. J Biol Chem 2000;275:14632–41.
47. Chen CC, Chen N, Lau LF. The angiogenic factors Cyr61 and connective tissue growth factor induce adhesive signaling in primary human skin fibroblasts. J Biol Chem 2001;276:10443–52.
48. Babic AM, Kireeva ML, Kolesnikova TV, Lau LF. CYR61, a product of a growth factor-inducible immediate early gene, promotes angiogenesis and tumor growth. Proc Natl Acad Sci U S A 1998;95: 6355–60.
49. Crean JK, Finlay D, Murphy M, et al. The role of p42/44 MAPK and protein kinase B in connective tissue growth factor induced extracellular matrix protein production, cell migration, and actin cytoskeletal rearrangement in human mesangial cells. J Biol Chem 2002;277:44187–94.

Integrated Transforming Growth Factor-β / Fibroblast Growth Factor-2 Signaling Regulates Reactive Stroma and Promotes Prostate Cancer

Feng Yang*, Douglas W. Strand* and David R. Rowley[1]

Department of Molecular and Cellular Biology,

Baylor College of Medicine,

One Baylor Plaza,

Houston, TX 77030

* Denotes equal contribution by these authors. [1]To whom requests for reprints should be addressed: Department of Molecular and Cellular Biology, Baylor College of Medicine, Houston, TX 77030. Phone: (713) 798-6220; Fax: (713) 790-1275; E-mail: drowley@bcm.tmc.edu.

Running Title: TGF-β signaling in prostate cancer reactive stroma.

Key Words: Transforming growth factor beta, fibroblast growth factor, prostate cancer, stroma, angiogenesis

This work was supported by NIH grants, RO1-CA058093, RO1-DK045909, SPORE P50-CA58204, UO1-CA84296, and Department of Defense grant W81XWH-04-1-0189, PC030817.

Abstract

Transforming growth factor-β (TGF-β) is overexpressed at sites of wound repair and in most adenocarcinomas including prostate cancer. In stromal tissues, TGF-β regulates cell proliferation, phenotype, and matrix synthesis. Our previous studies suggest reactive stroma promotes prostate cancer tumorigenesis, however, the mechanisms of TGF-β action in cancer-associated reactive stroma are not well understood. To address mechanisms, we developed prostate stromal cells null for TGF-β receptor II (TβRII) or engineered to express a dominant negative Smad3 (Smad3ΔSSVS) to attenuate TGF-β signaling. The DRS (differential reactive stroma) xenograft model was used to evaluate altered stromal TGF-β signaling on LNCaP tumor progression. LNCaP xenograft tumors constructed with TβRII null stromal cells exhibited a 49.8% reduction in mass relative to controls. Similarly, stromal expression of Smad3ΔSSVS resulted in a 40.6% decrease in tumor mass. Significantly lower microvessel density and decreased cellular fibroblast growth factor-2 (FGF-2) immunostaining were associated with attenuated TGF-β signaling in stroma. *In vitro*, TGF-β stimulated stromal FGF-2 expression and release. However, stromal cells with attenuated TGF-β signaling exhibited low basal FGF-2 expression and were refractory to TGF-β stimulated FGF-2 expression and release. Re-expression of FGF-2 in these stromal cells in DRS xenografts resulted in restored tumor mass and microvessel density. These data show that TGF-β signaling in reactive stroma is tumor-promoting and that this effect is mediated in part through a TβRII/Smad3-dependent up-regulation of FGF-2 expression and release. Accordingly, TGF-β/FGF-2 signaling in cancer-associated reactive stroma is likely a key mechanism through which the microenvironment promotes angiogenesis and tumorigenesis.

Introduction

Several studies suggest that the generation of a reactive stromal microenvironment regulates carcinoma progression, however, the specific biological functions of reactive stroma and the key factors and signaling mechanisms that mediate a tumor regulatory function of reactive stroma are not well understood. TGF-β has emerged as a key candidate for regulation of the tumor microenvironment due to its critical function in modulating stromal cell phenotype and promoting angiogenesis. TGF-β regulates diverse functions of stromal cells through both Smad-dependent and -independent signaling pathways and is a key regulator of stromal cells at sites of wound repair and fibrosis (1-3). Using Smad3 knockout mice, studies have shown that TGF-β-induced fibrosis is partly mediated through Smad3 pathways, although it is less clear whether this pathway or others are activated in stromal cells during wound healing and in carcinoma-associated reactive stroma (4, 5).

Our previous studies have shown that reactive stroma initiates directly adjacent to foci of pre-malignant prostatic intraepithelial neoplasia (PIN) and subsequently co-evolves with human prostate cancer progression (6). This reactive stroma is composed of both activated fibroblasts and myofibroblasts and elevated TGF-β1 was observed in PIN epithelial cells. Concordantly, TGF-β1 induced human prostate stromal cells in culture to a myofibroblast phenotype that overexpressed tenascin, a biomarker of reactive stroma (6). Using differential cDNA microarray analyses, we subsequently showed that connective tissue growth factor (CTGF) was expressed at low levels in nontumor-promoting prostate stromal cells. Moreover, in addition to the TGF-β-induced stromal CTGF expression observed in culture, ectopic stromal CTGF expression promoted LNCaP differential reactive stroma (DRS) xenograft tumor growth and angiogenesis suggesting that CTGF may be a downstream mediator of TGF-β action in cancer-associated

reactive stroma(7). In general, TGF-β is overexpressed in most human carcinomas that are associated with a reactive stroma (8-10) and is thought to promote cancer progression. However, under variant conditions, some reports have indicated that TGF-β may inhibit cancer progression which demonstrates the need to define, in a tumor-specific context, the specific mechanisms and mediators of TGF-β action in reactive stroma and whether this results in a cancer-promoting or –inhibiting biology (11-14).

Reactive stroma that forms in response to carcinoma is phenotypically similar to a wound repair stroma (15, 16). In wound repair, TGF-β stimulates extracellular matrix deposition, regulates stromal cell phenotype, and is pro-angiogenic (2, 17, 18). One of the angiogenic molecules transiently regulated by TGF-β during wound repair is fibroblast growth factor 2 (FGF-2) (19, 20). In addition to its angiogenic role, FGF-2 is also mitogenic for stromal and epithelial cells, and is significantly up-regulated in prostatic disease (21, 22). Accordingly, it has been suggested that growth factor expression in reactive stroma promotes carcinoma progression (23-25).

In this report, we show that attenuated TGF-β signaling in prostate stromal cells through either a targeted knockout of TGF-β receptor II (TβRII) or by expression of a dominant negative Smad3 results in an inhibition of the tumor-promoting function of reactive stroma in the human prostate cancer DRS xenograft model. In addition, we show that the pro-angiogenesis and tumor-promoting function of TGF-β signaling in this model is mediated, in part, by induced expression and release of FGF-2 from reactive stromal cells in a TβRII/Smad3-dependent manner.

Materials and Methods

Cell Lines. LNCaP human prostate carcinoma cells were purchased from ATCC (American Type Culture Collection, Manassas, VA) and maintained in RPMI 1640 media (Invitrogen, Carlsbad, CA) supplemented with 10% fetal bovine serum (FBS) (Hyclone, Logan, UT), 100 Units/ml penicillin, and 100 μg/ml streptomycin (Sigma, St Louis, MO). The Phoenix E packaging cell line was obtained from ATCC by permission from Dr. Gary Nolan (Stanford University) and maintained in DMEM with high glucose (Invitrogen) supplemented with 10% heat inactivated FBS (Hyclone), 2 mM glutamine (Invitrogen), 100 units/ml penicillin, and 100 μg/ml streptomycin (Sigma). The C57B mouse prostate stromal cell line was generated as reported previously (7) and cultured in Bfs medium: DMEM (Invitrogen) supplemented with 5% FBS (Hyclone), 5% Nu Serum (BD Biosciences, Bedford, MA), 0.5 μg/ml testosterone, 5 μg/ml insulin, 100 units/ml penicillin and 100 μg/ml streptomycin (Sigma).

We established the PSTΔRII$^{flox/flox}$H prostate stromal cell line from the ventral prostate of an 8 week Tgfbr2$^{floxE2/floxE2}$ mouse that was kindly provided by Dr. Neil Bhowmick (Vanderbilt University) (12). The ventral prostate was cut into approximately 1 mm^3 pieces and placed in a 12 well culture plate in Bfs media. Primary cultures of stromal cells reached confluence and were passaged and maintained in Bfs media and thereafter referred to as a finite cell line according to conventional terminology (The Society for In Vitro Biology). Cultures at passages 8–15 were used for all experiments.

Knockout of *TβRII* alleles in PSTΔRII$^{flox/flox}$H cells. The self-excising "Hit and Run" HR-MMPCreGFP retroviral construct containing cDNA encoding an active Cre-GFP fusion protein with a *lox* 511 in the 3' LTR U3 region, and the control construct HR-MMPCreGFPY324F containing cDNA encoding CreY324F-GFP fusion protein (a loss of function Cre Recombinase mutant), were kindly provided by Drs. Daniel P. Silver and David M.

Livingston (Harvard University) (26). These constructs were transfected into Phoenix E cells with the Calcium Phosphate Transfection kit (Invitrogen), following procedures published previously (7). Virus was collected, filtered (0.45 μm) and applied to infect PSTΔRII$^{flox/flox}$H stromal cells as previously described (7). Expression of the Cre-GFP fusion protein in PSTΔRII$^{flox/flox}$H cells excised the floxed *TβRII* alleles and self-excised the lox 511 flanked *CreGFP*, resulting in TβRII null prostate stromal cells termed PSTΔRIIKO cells. Expression of CreY324F-GFP in PSTΔRII$^{flox/flox}$H cells did not excise *TβRII* alleles and these control cells were named PSTΔRIICT. The *TβRII* knockout efficiency in the PSTΔRIIKO cells was determined by biological assays using TGF-β responsive reporter assays and TGF-β-induced smooth muscle α-actin (SM-ααactin) filament formation as described below.

N-Flag-Smad3ΔSSVS expression in C57B prostate stromal cells. To inhibit Smad3-mediated signaling pathways, either pLPCX-N-Flag-Smad3ΔSSVS or control vector pLPCX, kindly provided by Drs. Lisa Choy Tomlinson and Rik Derynck (University of California, San Francisco), was transfected into Phoenix E cells with a Calcium Phosphate Transfection kit (Invitrogen). Virus was collected, filtered (0.45 μm) and applied to infect C57B mouse prostate stromal cells following a previously described protocol (7). Cells were cultured in Bfs media and selected using 2 μg/ml puromycin. The resulting cell lines were termed C57B-Smad3ΔSSVS and control C57B-Ctrl cells. Infected cells were evaluated for expression of the dominant negative Smad3 construct by immunofluorescence (Flag-tag) as described below. C57B-Smad3ΔSSVS cells were tested for attenuated Smad3 signaling using a Smad3-responsive reporter assay as described below.

Immunofluorescence. For detection of N-Flag-Smad3ΔSSVS expression, C57B-Ctrl and C57B-Smad3ΔSSVS cells were cultured in Bfs media on coverslips to 50% confluence,

washed briefly in PBS, fixed with methanol for 10 min and acetone for 1 min at –20 ^{0}C. After blocking in 1% BSA in PBS, the cells were sequentially incubated with rabbit anti-Flag antibody (1:200, Sigma), FITC-conjugated goat anti-rabbit IgG (1:150, Jackson ImmunoResearch Laboratories Inc, West Grove, PA) and mounted with VECTASHIELD mounting media with DAPI (Vector Laboratories Inc., Burlingame, CA). Cells were examined and photographed with a Nikon fluorescence microscope.

For detection of SM-α-actin filament formation, TβRIIKO and TβRIICT cells were cultured on coverslips in Bfs media to 20% confluence, followed by exposure to 50 pM of TGF-β1 or vehicle control in M0 (MCDB 110 supplemented with insulin, tranferrin, and sodium selenite (Sigma Diagnostics)) media for 72h. The cells were then washed briefly in PBS, fixed in 4% paraformaldehyde (neutral buffered) at room temperature for 10 min, and washed sequentially in PBS and PBS with 0.1% Triton X-100. After blocking in 1% BSA in PBS, the cells were immunostained for SM-α-actin (FITC-conjugated anti-SM-α-actin, Sigma) as described previously (6).

Promoter Assays. The PSTβRIIKO, PSTβRIICT, PSTβRII$^{flox/flox}$H, C57B-Ctrl and C57B-Smad3ΔSSVS cells were seeded into 12 well plates at a density of 1×10^4 cells/cm^2 and incubated at 37 ^{o}C overnight. One hour before transfection, the cells were switched to DMEM with 0.2% FBS. The cells were then transfected with 0.4 μg/well of either p800Luc (27), (CAGA)$_{12}$MLP (28), α-SMAp-luc (29) or pVim-luc (a reporter construct made in pGl3 vector (Promega Corp. Madison, WI) containing PCR amplified –825 to –28 human vimentin promoter region from –757Cat (30)) with FuGENE 6 transfection reagent according to the manufacturer's protocol (Roche Applied Sciences, Indianapolis, IN). A promoter-less pRL-null vector (Promega) co-transfected at 0.1 μg/well was used for an internal transfection efficiency control.

Medium was replaced 24h after transfection with fresh DMEM containing 0.2% FBS with 50 pM of TGF-β1 (R&D Systems, Minneapolis, MN) or vehicle control. Cells were collected 24h later and assayed for luciferase activity using the Dual-Luciferase® Reporter Assay system (Promega) following the manufacturer's protocol with a luminometer. The luciferase activity was normalized to the co-transfected pRL-null and expressed in relative units or fold induction.

TGF-β1-regulated FGF-2 Message in prostate stromal cells (qPCR). Transcriptional regulation of native FGF-2 message by TGF-β1 was assessed by quantitative reverse transcription-polymerase chain reaction (RT-PCR). PSTΔRIICT, PSTΔRIIKO, C57B-Ctrl and C57B-Smad3ΔSSVS prostate stromal cells were seeded in 6-well plates at 2 x 10^5 cells/well in Bfs medium for 24 hours upon which media was changed to 0.5% FBS in DMEM for 24 hours to induce quiescence. Cells were then treated with 100 pM (2.5ng/ml) porcine TGF-β1 (R&D Systems) or vehicle control in 0.5% FBS in DMEM for 24 hours and total RNA was extracted using the RNeasy Miniprep kit (Qiagen, Inc., Valencia, CA). 1μg total RNA was reverse transcribed with random hexamer primers using the SuperScript III First Strand Synthesis kit (Invitrogen, Carlsbad, CA) for 50 min at 50°C in a 100-μl reaction volume according to the manufacturer's instructions. Then 1μl of reversed transcribed product was analyzed for mouse FGF-2 and GAPDH by real-time PCR using Platinum SYBR Green qPCR SuperMix-UDG with ROX (Invitrogen) on the ABI Prism PE7700 sequence analyzer (Applied Biosystems, Foster City, CA). Gene-specific PCR primers were designed using Primer Express software (Applied Biosystems) following the guidelines provided by Applied Biosystems. The FGF-2 amplicon spanned exons 1 and 2 and consisted of the primers 5'GTCCGCGAGAAGAGCGAC (T_m = 59°C) and 5'ACACTCCCTTGATAGACACAACTCC (T_m = 59°C). For an internal control, a GAPDH amplicon was designed to span exons 5 and 6 and consisted of the primers 5'

CCTACCCCCAATGTGTCCG (T_m = 59°C) and 5' CCTTCTTGATGTCATCATACTTGGC (T_m = 59°C). Amplification was performed using MicroAmp 96-well plates with 10 μM primers in a 25 μl reaction volume. The thermal cycling conditions were AmpErase UNG activity for 2 min at 50°C, Platinum *Taq* DNA polymerase activation for 10 min at 95°C, and 40 cycles of 15 s at 95°C and 30 s at 60°C. Cycle threshold values (Ct) were analyzed using SDS1.9 software (Applied Biosystems). Singleplex FGF-2 quantities were normalized against GAPDH RNA amplification. Relative expression levels were determined by the comparative Ct method (*ABI Prism 7700 SDS User Bulletin no. 2;* Applied Biosystems). The slope of log input amount versus ΔCt was 0.05, indicating similar amplification efficiencies of FGF-2 and the GAPDH RNA reference.

Ectopic FGF-2 expression in PSTΔRIIKO and C57B-Smad3ΔSSVS cells. The pRev-TRE2 vector containing the 18kDa FGF-2 isoform with C-terminal fusion to GFP was kindly provided by Dr. Walter Nickel (Heidelberg University, Germany) (31). FGF-2-GFP cDNA was excised from pRev-TRE2 with EcoRI digestion and ligated into the retroviral vector pBMN-LacZ kindly provided by Dr. Gary Nolan (Stanford University). The FGF-2 cDNA orientation and sequence was verified by sequencing. Functionality of the FGF-2 fusion protein has been established previously (31). Either pBMN-FGF-2-GFP or control vector pBMN-I-eGFP (Dr. Gary Nolan) was transfected into Phoenix E cells, virus was collected, filtered (0.45 μm) and applied to infect PSTΔRIIKO or C57B-Smad3ΔSSVS mouse prostate stromal cells as described above. The resulting cell lines were named PSTΔRIIKO-FGF-2, PSTΔRIIKO-Ctrl, C57B-Smad3ΔSSVS-FGF2 and C57B-Smad3ΔSSVS-Ctrl. Expression of the retroviral construct was confirmed by counting the percentage of green fluorescent (GFP positive) cells per X100 field. Infected cultures with a >90% green fluorescent cells per field were passaged and frozen (-80°C)

in 4 x 10^6 cells/vial aliquots for direct use in DRS xenografts as we have reported previously (7, 32). Expression of FGF-2 protein in cell lines and DRS xenografts was verified by Western blot and immunohistochemistry as described below. Quantitation of FGF-2 released into the conditioned media was evaluated by ELISA as described below.

ELISA (Quantitation of FGF-2 protein). For determination of native FGF-2 protein, PSTΔRIICT, PSTΔRIIKO, C57B-Ctrl and C57B-Smad3ΔSSVS cells were seeded at 2 X 10^5 cells/well in 6-well plates in Bfs media for 24 hours followed by washing with PBS and replacing media with 0.5% FBS in DMEM for 24 hours. Cultures were subsequently treated with 100 pM porcine TGF-β1 (R&D Systems) or vehicle control for 24 hours. Cell extracts were made in 250 μl/well RIPA buffer (150mM NaCl, 50mM Tris HCl, 0.5% DOC, 0.1% SDS, 1% NP-40, protease inhibitor cocktail (Sigma)).

For determination of FGF-2 released into the conditioned media, PSTΔRIICT, PSTΔRIIKO, C57B-Ctrl and C57B-Smad3ΔSSVS cells were infected with virus containing FGF-2-GFP as described in the previous section producing the PSTΔRIICT-FGF-2, PSTΔRIIKO-FGF-2, C57B-Ctrl-FGF-2, and C57B-Smad3ΔSSVS-FGF-2 cell lines. Cells expressing ectopic FGF-2 were seeded at 1 x 10^5 cells in 25 cm^2 flasks in Bfs for 24 hours followed by washing in PBS and replacing media with 1% FBS in DMEM for 24 hours. Cultures were subsequently treated with 4-40 pM porcine TGF-β1 or vehicle control for 24 hours and conditioned media was collected and centrifuged to remove debris. Both cellular FGF-2 (from 100 μl cell extracts) and released FGF-2 (from 100 μl conditioned media) were quantified by an FGF-2-specific ELISA following the manufacturer's protocol (R&D Systems) and normalized to total cell number.

Western blot. To detect recombinant FGF-2 protein by western blot, 10 μg of cell extract were electrophoresed through a 12% SDS-PAGE gel. Proteins were transferred onto Nitrocellulose membrane (Bio-Rad Laboratories, Hercules, CA) and incubated in PBS buffer with 5% milk at 4°C overnight. Membranes were probed with a rabbit anti-GFP antibody (1:2,000, Molecular Probes, Eugene, OR) for 1 hour at room temperature (RT), followed by incubation with a biotin-conjugated goat anti-rabbit IgG (1:10,000, Sigma) for 45 minutes at RT. A streptavidin-horseradish peroxidase conjugate (Amersham Pharmacia Biotech UK Ltd, Buckinghamshire, UK) diluted at 1:5,000 was incubated for 30 mins at RT. Protein bands were detected by incubation with ECL+plus Western blotting detection system (Amersham Biosciences, UK Ltd, Buckinghamshire, UK) for 5 min at room temperature followed by exposure to Hyperfilm™ ECL™ from Amersham Pharmacia Biotech UK Ltd.

Animals and Preparation of DRS Xenografts. Athymic NCr-*nu*/*nu* male homozygous nude mice, 6–8 weeks of age, were purchased from Charles River Laboratories (Wilmington, MA). All experiments were in compliance with the NIH Guide for the Care and Use of Laboratory Animals and according to the institutional guidelines of Baylor College of Medicine.

DRS xenografts were generated following procedures we have published previously (7, 32-34). Xenografts were generated as following: Briefly, 16 × 10^6 LNCaP cells were combined with 4 × 10^6 of either PSTΔRIICT, PSTΔRIIKO, C57B-Ctrl, C57B-SmadΔSSVS, PSTΔRIIKO-Ctrl, PSTΔRIIKO-FGF2, C57B-SmadΔSSVS-Ctrl, or C57B-SmadΔSSVS-FGF2 prostate stromal cells. Cells were washed once with 10 ml of RPMI 1640 containing 10% FBS in 15-ml conical tubes. The cells were centrifuged at 400g for 2 minutes and resuspended in 6 ml of the same media. The LNCaP cells were then combined with stromal cells, mixed well and centrifuged again at 400g for 2 minutes. The supernatant was aspirated to 300 μl. The cells

were transferred to the TMF mouse facility and gently resuspended. After incubation on ice for 90 seconds, the cells were combined and mixed thoroughly with cold 0.5 ml Matrigel (Becton Dickinson, Bedford, MA). The mixture was drawn into a 1-ml syringe fitted with a 20-gauge needle. After switching to a 25-gauge needle, 100 μl of cell suspension was injected subcutaneously per site in each rear lateral flank, two injections per mouse, 3 mice, for a total of 6 tumors per injection preparation. A minimum of 3 independent experiments was performed for each combination tested (n=18 tumors).

Xenograft tumors were evaluated at either day 14 or 28 post-inoculation as these are optimal intermediate and later stage time points to assess microvessel density and xenograft mass as we have reported previously (7, 32-34). Xenografts were weighed and fixed in 4% paraformaldehyde (neutral buffered) at 4°C overnight, washed 3× in PBS and paraffin-embedded. 5 μm sections were mounted onto ProbeOn Plus slides (Fisher Scientific, Pittsburgh, PA) and either stained with H&E for histological analysis or processed for immunohistochemistry.

Immunohistochemistry with DRS Xenografts. Immunostaining of CD31 was performed with the MicroProbe Staining System (Fisher Scientific) following a protocol published previously (32). Anti-mouse CD31/PECAM-1 antibody and biotin-conjugated goat anti-rat IgG were from BD PharMingen (San Diego, CA). The protocol used for FGF-2 and GFP immunostaining followed a general protocol published previously (32). Briefly, after dewaxing, antigen retrieval was performed by steaming paraffin-embedded sections for 20 minutes in 10 mM citrate buffer. Sections were incubated with either a rabbit anti-GFP antibody (1:50, Molecular Probes) or a rabbit anti-FGF-2 antibody (1:200, Santa Cruz) for 1 hour at 37°C, washed, and incubated for 45 minutes at 37°C with a biotin-conjugated goat-anti-rabbit IgG

secondary antibody (1:800, Sigma, B-8895). Reagents formulated for use with capillary action systems were purchased from Open Biosystems (Huntsville, AL) and used according to the manufacturer's protocol.

Microvessel Density and Epithelial to Stromal Cell Ratio Analyses. Analysis was performed according to procedures we have reported previously with DRS xenografts (7, 32-34). For microvessel density analysis, tissue sections were stained for CD31 as described above. Vessels per 400X random fields were counted by an observer blinded to experimental conditions. The average vessel count was determined for each specimen. An n=12 xenografts with six random fields per tumor from each separate combination were analyzed. To determine epithelial to stromal cell ratios, H & E stained sections at 400X random fields were counted by a blinded observer for number of epithelial cells and stromal cells per field. An n=6 xenografts with 2 fields per xenograft from each combination were analyzed for each combination.

Statistical Analysis. Xenografts from each condition were analyzed, and mean xenograft mass and mean microvessel density counts were compared with values from matching control tumors for statistical relevance using the unpaired *t* test (two-tailed). Statistical analyses were generated using GraphPad Prism for Macintosh version 4.0 (GraphPad Software, San Diego, CA). $P < 0.05$ was considered statistically significant.

Results

Attenuation of TGF-β signaling in prostate stromal cell lines. To address the biological effect of TGF-β signaling within the stromal compartment on prostate cancer progression, an adult, differentiated prostate stromal cell line null for TβRII was generated. Briefly, primary stromal cell cultures were initiated from the ventral prostate of a C57B

Tgfbr2$^{floxE2/floxE2}$ mouse, which carries *loxP* sites at introns 1 and 2 of the TGF-β type II receptor (*TβRII*) gene as previously described by Bhowmick *et al* (12). Upon first passage these cultures were termed the PSTβRII$^{flox/flox}$H cell line. Retroviral-mediated expression of Cre-GFP (a functional Cre DNA recombinase-GFP fusion protein), in a "Hit and Run" pattern, was used to knock out floxed *TβRII* alleles and self-excise the *CreGFP* transgene to limit Cre-induced toxicity in the cells (26). Control cells received CreGFPY324F, a loss-of-function Cre DNA recombinase mutant (26). The resulting cell lines were termed PSTβRIIKO (Prostate Stromal cells-TβRII KnockOut) and PSTβRIICT (Prostate Stromal cells-TβRII ConTrol), respectively.

Compared with PSTβRIICT cells and the parent PSTβRII$^{flox/flox}$H cells, attenuated TGF-β signaling was observed in the PSTβRIIKO cells. In control cells, TGF-β1 (50 pM) stimulated a 7-8 fold expression of p800Luc (PAI-1 promoter) (27) (Figure 1*A*), a 3-fold expression of α-SMAp-luc (smooth muscle α-actin promoter) (29) (Figure 1*B*) and a 3-4 fold expression of pVim-luc (vimentin promoter) (Figure 1*C*). In contrast, there was no significant TGF-β1-induced promoter activity with any of these constructs in the PSTβRIIKO cells. TGF-β1 also induced a 250-270 fold expression of $(CAGA)_{12}$MLP (Smad binding sequence) (28) in control cell lines, whereas this induction was restricted to 2.6-fold in PSTβRIIKO cells (Figure 1*D*). Since TGF-β has been shown to induce SM-α-actin filament formation during myofibroblast and smooth muscle cell differentiation, we determined whether this effect was attenuated in PSTβRIIKO cells. Accordingly, TGF-β1 induced SM-α-actin filament formation in the control PSTβRIICT cells, but had no appreciable effect in PSTβRIIKO cells (Figure 2*A*,*B*).

Attenuated TGF-β signaling in stromal cells inhibits LNCaP DRS xenografts. To evaluate whether attenuated TGF-β signaling in prostate stroma affected tumorigenesis, xenografts were constructed by injecting human LNCaP cells together with PSTβRIIKO cells or

control PST□RIICT cells, each combined with B.D. Matrigel in male NCr-*nu*/*nu* mice following procedures we have reported previously (7, 32-34). Xenografts were evaluated at 28 days post-injection for changes in tumor mass, histopathology and microvessel density as we have reported previously (7, 32). As shown in Figure 2*C*, attenuated TGF-□ signaling in the PST□RIIKO cells resulted in a 49.8% decrease in the tumor mass of the LNCaP / PST□RIIKO xenografts (mean = 19.97 ± 2.77 mg, mean ± SEM) relative to control LNCaP / PST□RIICT xenografts (39.77 ± 7.36 mg, mean ± SEM) (P=0.0167, n=18 in each group) at day 28. Concordantly, a 44.1% reduction in microvessel density was observed in LNCaP / PST□RIIKO xenografts (8.49 ± 1.01, mean ± SEM) compared to control LNCaP / PST□RIICT xenografts (15.18 ± 0.96, mean ± SEM) (P<0.0001, n=72 fields, 12 tumors in each group) (Figure 2*D*). Histopathology of xenograft tumors showed clusters of LNCaP cells adjacent to reactive stroma and vessels similar to what we have reported previously for this model and no obvious histological differences were observed in experimental compared to control tumors (data not shown) (7, 32-34). Quantitative evaluation of cancer cell to stromal cell ratios showed there were no significant differences in the ratios of LNCaP carcinoma cells to stromal cells in experimental tumors relative to control (data not shown).

TGF-□ regulation of tumor-promoting stroma is partially mediated through FGF-2 signaling. Because of the decreased angiogenesis seen in tumors without stromal TGF-□ signaling, stromal cells were examined by immunohistochemistry for expression of FGF-2, an angiogenic growth factor expressed in stroma at sites of wound repair and cancer. Positive FGF-2 immunoreactivity was observed in stromal cells in LNCaP / PST□RIICT xenografts. In contrast, little to no immunoreactivity was observed in stromal cells of LNCaP / PST□RIIKO xenografts (Figure 3*A*), further suggesting the involvement of FGF-2 in the tumor-promoting

biology of TGF-β signaling. Quantitative RT-PCR and ELISA data validated the decreased FGF-2 immunoreactivity observed in xenograft tumors demonstrating that TβRII was required for the upregulation of FGF-2 mRNA and protein in cultured prostate stromal cells (Figure 3*B*,*C*, respectively). Finally, to determine whether TGF-β induced release of FGF-2, stromal cells were engineered to over-express the secreted 18kDa isoform of FGF-2 as a biologically active GFP fusion (32) using a retroviral infection as described in the Materials and Methods. Western blot results show that ectopic FGF-2 protein levels were comparable between the PSTβRIICT-FGF-2 and PSTβRIIKO-FGF-2 cells under these conditions (Figure 3*D*, inset). Treatment of control cells showed that TGF-β1 induced a significant, dose-dependent release of FGF-2 into conditioned media, whereas this effect was inhibited in PSTβRIIKO-FGF-2 cells under these conditions (Figure 3*D*).

To determine whether the tumor-inhibiting effects of attenuated TGF-β signaling in stromal cells could be attributed to decreased FGF-2 expression, xenografts were constructed with LNCaP cells plus either PSTβRIIKO engineered to over-express FGF-2-GFP (18kDa) or these cells with the empty control vector (PSTβRIIKO-FGF2 or PSTβRIIKO-Ctrl). LNCaP / PSTβRIIKO-FGF2 xenografts showed resumed stromal FGF-2 immunostaining (Figure 4*A*) and this was due to the expression of the FGF-2-GFP fusion protein as these cells were also positive for GFP (Figure 4*B*). Over-expression of FGF-2 under these conditions produced a 40.0% increase in xenograft tumor mass in LNCaP / PSTβRIIKO-FGF2 xenografts (20.98 ± 1.72 mg) compared to LNCaP / PSTβRIIKO-Ctrl xenografts at day 14 (14.99 ± 1.43 mg) (P=0.0127, unpaired t test, n=18 xenografts in each group) (data not shown). A 141.1% increase in xenograft tumor mass was observed in LNCaP / PSTβRIIKO-FGF2 xenografts (44.14 ± 5.82 mg) compared to LNCaP / PSTβRIIKO-Ctrl xenografts at day 28 (18.31 ± 1.01 mg) (P<0.0001,

unpaired *t* test, n=18 xenografts in each group) (Figure 4*C*). Additionally, LNCaP / PSTRIIKO-FGF2 xenografts exhibited a 38.9% elevation of microvessel density (10.50± 1.04) compared to control LNCaP / PSTRIIKO-Ctrl xenografts (7.56± 0.84) (*P*=0.0307, unpaired *t* test, n=72 fields, 12 xenografts in each group) (Figure 4*D*).

TGF- Regulation of Tumor-Promoting Stroma is Smad3-Mediated. The role of Smad3-mediated signaling in reactive stroma of cancer has not been addressed in previous studies. Accordingly, a key question of this study was to determine whether Smad3-mediated signaling is key in the tumor-promoting biology of cancer-associated stroma. We addressed this question using a dominant negative Smad3 (Smad3ΔSSVS) construct in C57B mouse prostate stromal cells to determine the effect that attenuating Smad3 signaling in stroma has on tumorigenesis. To attenuate Smad3 signaling, the C57B prostate stromal cell line was infected with either the vector control virus (pLPCX) or a virus containing dominant negative Smad3 (N-Flag-Smad3ΔSSVS) to create the C57B-Ctrl and C57B-Smad3ΔSSVS cell lines, respectively. This Smad3 dominant negative construct has been shown in previous studies to attenuate Smad3-mediated TGF- signaling (35). Expression of the Flag-Smad3ΔSSVS in C57B-Smad3ΔSSVS cells was verified by immunofluorescence using an antibody to the Flag tag (data not shown). Attenuation of Smad3 signaling was verified by a significant reduction in TGF-1-induced expression of the Smad3-responsive $(CAGA)_{12}$MLP reporter in the C57B-Smad3ΔSSVS cells compared to control (Figure 5*A*). Construction of DRS xenograft tumors with LNCaP epithelia and C57B-Smad3ΔSSVS stromal cells resulted in a significant reduction in xenograft tumor mass and microvessel density. LNCaP / C57B-Smad3ΔSSVS xenografts exhibited a 24.5% decrease in mean tumor mass at day 14 (21.48 ± 1.60 mg) as compared to control LNCaP / C57B-Ctrl xenografts (28.46 ± 1.21 mg) (*P*=0.0014, unpaired *t* test, n=18 tumors in each group)

(data not shown). A 40.6% decrease in mean wet weight was observed at day 28 in LNCaP / C57B-Smad3ΔSSVS xenografts (30.96 ± 4.52 mg) relative to control LNCaP / C57B-Ctrl tumors (52.09 ± 7.52 mg) (P=0.0216, unpaired t test, n=18 xenografts in each group) (Figure 5*B*). Alteration in tumor mass was associated with reduced microvessel density as LNCaP / C57B-Smad3ΔSSVS xenografts exhibited a 31.4% decrease in mean microvessel density (10.60 ± 1.33) compared to control LNCaP/C57B-Ctrl xenografts (15.46 ± 1.26) (P=0.0089, unpaired t test, n=72 fields, 12 xenografts in each group) (Figure 5*C*). Consistent with xenografts constructed with TβRII null stromal cells, there were no other significant differences in cancer cell to stromal cell ratios or obvious changes in histopathology (data not shown).

Smad3-Regulated FGF-2 expression in prostate stromal cells is tumor-promoting. An additional key question of this study is whether FGF-2 expression in stromal cells is Smad3-mediated as this has not been addressed in previous studies. Evaluation of C57B-Ctrl and C57B-Smad3ΔSSVS stromal cell lines *in vitro* showed that TGF-β1 (100 pM) stimulated FGF-2 mRNA in control cells but an attenuated response was observed in C57B-Smad3ΔSSVS cells (Figure 5*D*). Similarly, total cellular FGF-2 protein was significantly elevated in C57B-Ctrl cells stimulated with TGF-β1, whereas this effect was abrogated in C57B-Smad3ΔSSVS cells (Figure 6*A*). In addition, a significant release of FGF-2 into the conditioned media was observed in TGF-β1-treated C57B-Ctrl-FGF-2 cells, but not in C57B-Smad3ΔSSVS-FGF-2 cells, both of which ectopically expressed equivalent levels of 18kDa FGF-2-GFP (Figure 6*B*).

To determine whether the tumor-inhibiting effects of attenuated Smad3 signaling in stromal cells could be attributed in part to decreased FGF-2 expression, we over-expressed FGF-2 in C57B-Smad3ΔSSVS cells and constructed LNCaP DRS xenografts. Over-expression of FGF-2 produced a 30.4% increase in LNCaP /C57B-Smad3ΔSSVS-FGF-2 xenografts (24.15 ±

1.76 mg) compared to LNCaP / C57B-Smad3ΔSSVS-Ctrl control xenografts at day 14 (18.52 ± 1.27 mg, *P*=0.0138, unpaired *t* test, n=18 xenografts in each group) (Figure 6*C*). FGF-2-induced xenograft mass is comparable to day 14 control LNCaP / C57B-Ctrl xenografts with intact Smad3 signaling (28.46 ± 1.21 mg). Furthermore, LNCaP / C57B-Smad3ΔSSVS-FGF-2 xenograft tumors exhibited a 45.3% elevation in microvessel density (9.01 ± 0.69) compared to control xenografts (6.20 ± 0.60, *P*=0.0027, unpaired *t* test, n=72 fields, 12 xenografts in each group) (Figure 6*D*).

Discussion

Data presented here represent the first direct experimental evidence that links TGF-β action in the stromal compartment with the tumor-promoting biology of reactive stroma in prostate cancer. Furthermore, these data suggest that the biological actions of TGF-β signaling in reactive stroma is mediated in part through stimulated expression and release of FGF-2. Integrated TGF-β/FGF-2 signaling in stroma resulted in an elevated rate of prostate cancer tumorigenesis, consistent with a pro-angiogenic activity. In addition, these data show for the first time that TGF-β receptor signaling in cancer-associated reactive stroma is mediated, in part, through the Smad3 pathway, since signaling through additional pathways such as the MAP kinase pathways cannot be ruled out. These results are consistent with our previous reports, which have suggested that TGF-β induces a tumor-promoting reactive stroma in prostate cancer and a differentiation of adult human prostate stromal cells to a myofibroblast phenotype (6, 33). The identification of myofibroblasts in tumor-associated reactive stroma is reported in most human carcinomas (6, 23, 25, 36) and most carcinoma epithelial cells over-express TGF-β1 (8-

10, 24). Reactive stroma in human carcinomas has been characterized as a cancer-associated type of granulation tissue, which displays a myofibroblast phenotype similar to that observed in wound repair (15, 23, 24). Elevated angiogenesis, coordinate with elevated FGF-2 is common in granulation tissue and it is well established that TGF-β promotes granulation tissue formation and angiogenesis *in vivo* (2). FGF-2 is TGF-β-regulated and a mitogen for epithelial and stromal cells while also playing a role in the migration of endothelial cells during blood vessel formation. In addition to its fibrogenic role during wound repair, a significant upregulation of FGF-2 is seen in a variety of cancers including prostate cancer (21, 37, 38). Concordantly, tumor growth in the TRAMP mouse prostate cancer model was slowed in a FGF-2 knockout background (39). In addition, FGF receptor 1 (FGFR1), a cognate receptor for FGF-2, is upregulated in epithelia during prostate cancer progression in human cancer (21) and in mouse prostate cancer models (40). Therefore, it is likely that a TGF-β1-regulated and Smad3-mediated expression and release of FGF-2 in reactive stroma provides a pro-angiogenic and pro-tumorigenic microenvironment. Accordingly, the TGF-β/FGF-2 signaling axis is likely to be a key regulatory component of carcinoma cell – stromal cell homeostasis.

Acknowledgements

We thank Drs. Neil Bhowmick and Harold Moses for providing prostate tissue from a Tgfbr2$^{floxE2/floxE2}$ mouse, Drs. Daniel Silver and David Livingston for providing HR-MMPCreGFP and HR-MMPCreGFPY324F vectors, Drs Lisa Choy Tomlinson and Rik Derynck for providing pLPCX-N-Flag-Smad3ΔSSVS and pLPCX vectors, Dr. Gary Nolan for permission to use Phoenix E cells, and providing pBMN-LacZ and pBMN-I-eGFP vectors, and Dr. Walter Nickel for providing the pRev-TRE2-FGF2-GFP vector. We thank Dr. Sem Phan for providing the β-

SMAp-luc vector, Drs. Zendra Zehner and Susan Rittling for the –757Cat vector, Dr. David Loskutoff for the p800Luc vector, and Drs. Sylviane Dennler and Stephanie Huet for the $(CAGA)_{12}$MLP vector. We also thank Ms. Liz Hopkins for histological preparation of tissue, Mr. Truong Dang for maintenance of cell cultures, and Dr. Lisa Choy Tomlinson, Dr. Steven Ressler and Isaiah Schauer for helpful discussions.

References

1. Roberts AB and Sporn MB Transforming growth factor-β. In: Clark RAF editor, The Molecular and Cellular Biology of Wound Repair. New York, NY: Plenum Press; 1996. p. 275-308.
2. Roberts AB, Sporn MB, Assoian RK, *et al*. Transforming growth factor type beta: rapid induction of fibrosis and angiogenesis in vivo and stimulation of collagen formation in vitro. Proc Natl Acad Sci U S A 1986;83:4167-71.
3. Derynck R and Zhang YE. Smad-dependent and Smad-independent pathways in TGF-beta family signalling. Nature 2003;425:577-84.
4. Flanders KC, Major CD, Arabshahi A, *et al*. Interference with transforming growth factor-beta/ Smad3 signaling results in accelerated healing of wounds in previously irradiated skin. Am J Pathol 2003;163:2247-57.
5. Flanders KC. Smad3 as a mediator of the fibrotic response. Int J Exp Pathol 2004;85:47-64.
6. Tuxhorn JA, Ayala GE, Smith MJ, *et al*. Reactive stroma in human prostate cancer: induction of myofibroblast phenotype and extracellular matrix remodeling. Clin Cancer Res 2002;8:2912-23.
7. Yang F, Tuxhorn JA, Ressler SJ, *et al*. Stromal expression of connective tissue growth factor promotes angiogenesis and prostate cancer tumorigenesis. Cancer Res 2005;65:8887-95.
8. Barrett-Lee P, Travers M, Luqmani Y, *et al*. Transcripts for transforming growth factors in human breast cancer: clinical correlates. Br J Cancer 1990;61:612-7.
9. Coffey RJ, Jr., Shipley GD, and Moses HL. Production of transforming growth factors by human colon cancer lines. Cancer Res 1986;46:1164-9.
10. Eastham JA, Truong LD, Rogers E, *et al*. Transforming growth factor-beta 1: comparative immunohistochemical localization in human primary and metastatic prostate cancer. Lab Invest 1995;73:628-35.
11. Akhurst RJ and Derynck R. TGF-beta signaling in cancer--a double-edged sword. Trends Cell Biol 2001;11:S44-51.
12. Bhowmick NA, Chytil A, Plieth D, *et al*. TGF-beta signaling in fibroblasts modulates the oncogenic potential of adjacent epithelia. Science 2004;303:848-51.
13. Cheng N, Bhowmick NA, Chytil A, *et al*. Loss of TGF-beta type II receptor in fibroblasts promotes mammary carcinoma growth and invasion through upregulation of TGF-alpha-, MSP- and HGF-mediated signaling networks. Oncogene 2005;24:5053-68.
14. Wakefield LM and Roberts AB. TGF-beta signaling: positive and negative effects on tumorigenesis. Curr Opin Genet Dev 2002;12:22-9.
15. Dvorak HF. Tumors: wounds that do not heal. Similarities between tumor stroma generation and wound healing. N Engl J Med 1986;315:1650-9.
16. Gregoire M and Lieubeau B. The role of fibroblasts in tumor behavior. Cancer Metastasis Rev 1995;14:339-50.
17. Desmouliere A, Geinoz A, Gabbiani F, *et al*. Transforming growth factor-beta 1 induces alpha-smooth muscle actin expression in granulation tissue myofibroblasts and in quiescent and growing cultured fibroblasts. J Cell Biol 1993;122:103-11.

18. Massague J. The transforming growth factor-beta family. Annu Rev Cell Biol 1990;6:597-641.
19. Song QH, Klepeis VE, Nugent MA, *et al*. TGF-beta1 regulates TGF-beta1 and FGF-2 mRNA expression during fibroblast wound healing. Mol Pathol 2002;55:164-76.
20. Story MT, Hopp KA, and Meier DA. Regulation of basic fibroblast growth factor expression by transforming growth factor beta in cultured human prostate stromal cells. Prostate 1996;28:219-26.
21. Giri D, Ropiquet F, and Ittmann M. Alterations in expression of basic fibroblast growth factor (FGF) 2 and its receptor FGFR-1 in human prostate cancer. Clin Cancer Res 1999;5:1063-71.
22. Ozen M, Giri D, Ropiquet F, *et al*. Role of fibroblast growth factor receptor signaling in prostate cancer cell survival. J Natl Cancer Inst 2001;93:1783-90.
23. Ronnov-Jessen L, Petersen OW, and Bissell MJ. Cellular changes involved in conversion of normal to malignant breast: importance of the stromal reaction. Physiol Rev 1996;76:69-125.
24. Rowley DR. What might a stromal response mean to prostate cancer progression? Cancer Metastasis Rev 1999;17:411-9.
25. Tuxhorn JA, Ayala GE, and Rowley DR. Reactive stroma in prostate cancer progression. J Urol 2001;166:2472-83.
26. Silver DP and Livingston DM. Self-excising retroviral vectors encoding the Cre recombinase overcome Cre-mediated cellular toxicity. Mol Cell 2001;8:233-43.
27. Keeton MR, Curriden SA, van Zonneveld AJ, *et al*. Identification of regulatory sequences in the type 1 plasminogen activator inhibitor gene responsive to transforming growth factor beta. J Biol Chem 1991;266:23048-52.
28. Dennler S, Itoh S, Vivien D, *et al*. Direct binding of Smad3 and Smad4 to critical TGF beta-inducible elements in the promoter of human plasminogen activator inhibitor-type 1 gene. Embo J 1998;17:3091-100.
29. Hu B, Wu Z, and Phan SH. Smad3 mediates transforming growth factor-beta-induced alpha-smooth muscle actin expression. Am J Respir Cell Mol Biol 2003;29:397-404.
30. Rittling SR and Baserga R. Functional analysis and growth factor regulation of the human vimentin promoter. Mol Cell Biol 1987;7:3908-15.
31. Backhaus R, Zehe C, Wegehingel S, *et al*. Unconventional protein secretion: membrane translocation of FGF-2 does not require protein unfolding. J Cell Sci 2004;117:1727-36.
32. Tuxhorn JA, McAlhany SJ, Dang TD, *et al*. Stromal cells promote angiogenesis and growth of human prostate tumors in a differential reactive stroma (DRS) xenograft model. Cancer Res 2002;62:3298-307.
33. Tuxhorn JA, McAlhany SJ, Yang F, *et al*. Inhibition of TGF-β activity decreases angiogenesis in a human prostate cancer reactive stroma xenograft model. Cancer Res 2002;62:6021-5.
34. McAlhany SJ, Ressler SJ, Larsen M, *et al*. Promotion of angiogenesis by ps20 in the differential reactive stroma prostate cancer xenograft model. Cancer Res 2003;63:5859-65.
35. Choy L, Skillington J, and Derynck R. Roles of autocrine TGF-beta receptor and Smad signaling in adipocyte differentiation. J Cell Biol 2000;149:667-82.
36. Ronnov-Jessen L, Petersen OW, Koteliansky VE, *et al*. The origin of the myofibroblasts in breast cancer. Recapitulation of tumor environment in culture unravels diversity and

implicates converted fibroblasts and recruited smooth muscle cells. J Clin Invest 1995;95:859-73.
37. Dow JK and deVere White RW. Fibroblast growth factor 2: its structure and property, paracrine function, tumor angiogenesis, and prostate-related mitogenic and oncogenic functions. Urology 2000;55:800-6.
38. Bikfalvi A, Klein S, Pintucci G, *et al*. Biological roles of fibroblast growth factor-2. Endocr Rev 1997;18:26-45.
39. Polnaszek N, Kwabi-Addo B, Peterson LE, *et al*. Fibroblast growth factor 2 promotes tumor progression in an autochthonous mouse model of prostate cancer. Cancer Res 2003;63:5754-60.
40. Huss WJ, Barrios RJ, Foster BA, *et al*. Differential expression of specific FGF ligand and receptor isoforms during angiogenesis associated with prostate cancer progression. Prostate 2003;54:8-16.

Figure Legends

Figure 1. Retroviral mediated HR-CreGFP expression in PSTBRII $^{flox/flox}$ H cells efficiently blocks TGF-β1-induced signaling. TGF-β-responsive promoters, including (*A*) p800Luc, (*B)* β-SMAp-luc, *(C)* pVim-Luc or *(D)* $(CAGA)_{12}$MLP were transfected into PSTβRIIKO, the control PSTβRIICT and the parent PSTβRII$^{flox/flox}$H prostate stromal cells (PSTβRIIflox). Cultures were then exposed to either vehicle control (-) or TGF-β1 (50 pM) (+) for 24 hr and assayed for luciferase activity, which was normalized to the co-transfected pRL-null expressed Renilla luciferase activity. Data shown is mean ± SEM derived from replicate independent experiments. * = significant difference (P <0.05).

Figure 2. Attenuation of TGF-β signaling in stromal cells inhibits angiogenesis and rate of tumorigenesis in the LNCaP / prostate stromal cell DRS xenograft model. *A,* TGF-β1 induced formation of SM-α-actin filament in control PSTβRIICT cells. *B,* Attenuation of TGF-β signaling in PSTβRIIKO cells resulted in loss of TGF-β1-induced formation of SM-α-actin filaments. *Bar*, 50 μm. *C,* A significant decrease in tumor weight was observed at day 28 in LNCaP / TβRIIKO xenografts relative to control LNCaP / PSTβRIICT xenografts (P=0.0167, n=18 xenografts in each group). *D,* LNCaP / TβRIIKO xenografts exhibited a significant decrease in the mean microvessel density compared to control LNCaP / PSTβRIICT xenografts (P<0.0001, n=72 fields, 12 tumors in each group). * = significant difference.

Figure 3. TGF-β1 induces FGF-2 expression and release in prostate stroma. *A,* qRT-PCR showed an up-regulation of FGF-2 mRNA in TGF-β1-treated PSTβRIICT cells, but not in PSTβRIIKO cells. Similarly, ELISA results showed a significant increase in FGF-2 protein

levels in TGF-β1-treated PSTΔRIICT cells, but not in PSTΔRIIKO cells ($P = 0.0166$, n = 3 independent experiments). *B,* PSTΔRIICT and PSTΔRIIKO cells were infected to express equal levels of FGF-2-GFP, as shown by Western blot (anti-GFP, inset). ELISA experiments revealed a significant increase in FGF-2 protein released from TGF-β1-treated PSTΔRIICT-FGF-2 cells in a dose-dependent manner, whereas this response was inhibited in PSTΔRIIKO-FGF-2 cells ($P = 0.0471$, n = 3 independent experiments). * = significant difference. Immunohistochemistry revealed positive FGF-2 staining in (*C*) PSTΔRIICT cells, but little to no immunoreactivity was observed in (*D*) PSTΔRIIKO cells in DRS xenograft tumors (400X). Clusters of immunoreactive cells are LNCaP epithelia and arrows point to stromal cells surrounding epithelia.

Figure 4. Ectopic expression of FGF-2 in stromal cells with attenuated TGF-β signaling restored angiogenesis and tumorigenesis in LNCaP DRS xenografts. Expression of an FGF-2-GFP fusion protein in PSTΔRIIKO prostate stromal cells was verified by immunohistochemistry with (*A*) anti-FGF-2 and (*B*) anti-GFP antibodies (400X). *C,* LNCaP DRS xenograft tumors constructed with PSTΔRIIKO cells expressing FGF-2 display a significant increase in tumor mass compared to control xenografts at day 28 ($P<0.0001$, unpaired *t* test, n=18 xenografts in each group). *D,* Concordantly, microvessel density was significantly elevated in PSTΔRIIKO-FGF-2 xenografts compared to PSTΔRIIKO-CT xenografts ($P=0.0307$, unpaired *t* test, n=72 fields, 12 xenografts in each group). * = significant difference.

Figure 5. TGF-β-regulated xenograft tumorigenesis is partially mediated by Smad3. *A,* Immunofluorescence using a Flag antibody showed Flag-Smad3ΔSSVS expression in C57B-Smad3ΔSSVS cells, but not C57B-Ctrl cells. *Bar*, 50 μm. *B,* C57B-Smad3ΔSSVS cells showed a

significant decrease in TGF-β1-induced $(CAGA)_{12}$MLP reporter activity compared to C57B-Ctrl cells ($p<0.05$). *C,* A significant decrease in tumor weight was observed at day 28 in LNCaP / C57B-Smad3ΔSSVS xenografts relative to control LNCaP / C57B-Ctrl tumors (*P*=0.0216, unpaired *t* test, n=18 xenografts in each group). *D,* LNCaP / C57B-Smad3ΔSSVS xenografts exhibited a significant decrease in mean microvessel density compared to control LNCaP/C57B-Ctrl xenografts (*P*=0.0089, unpaired *t* test, n=72 fields, 12 xenografts in each group). * = significant difference.

Figure 6. Smad3-regulated FGF-2 expression and release in prostate stromal cells is tumor-promoting. *A,* qRT-PCR showed an up-regulation of FGF-2 mRNA in C57B-Ctrl cells, and this regulation was attenuated in C57B-Smad3ΔSSVS cells. ELISA results showed a significant increase in FGF-2 protein levels in response to TGF-β1 in C57B-Ctrl cells, whereas attenuated Smad3 signaling in C57B-Smad3ΔSSVS cells prohibited this increase ($P < 0.0001$, n = 3 independent experiments). *B,* C57B-Ctrl and C57B-Smad3ΔSSVS cells were infected to express equal levels of FGF-2-GFP (anti-GFP Western blot, inset). ELISA experiments revealed a significant increase in FGF-2 protein released from TGF-β1-treated C57B-Ctrl-FGF-2 cells in a dose-dependent manner, whereas this response was inhibited in C57B-Smad3ΔSSVS-FGF-2 cells. (*P* = 0.0085, n = 3 independent experiments). *C,* LNCaP DRS xenograft tumors constructed with C57B-Smad3ΔSSVS-FGF-2 cells displayed a significant increase in tumor mass compared to C57B-Smad3ΔSSVS-Ctrl xenografts at day 14 (*P*=0.0138, unpaired *t* test, n=18 xenografts in each group). *D,* Concordantly, microvessel density was significantly elevated in C57B-Smad3ΔSSVS-FGF-2 xenografts compared to C57B-Smad3ΔSSVS-Ctrl

xenografts (P=0.0027, unpaired t test, n=72 fields, 12 xenografts in each group). * = significant difference.